Physics – Uspekhi **53** (2) 133 – 157 (2010)

REVIEWS OF TOPICAL PROBLEMS PACS numbers: 52.25.Dg, **52.80.–s**, 82.33.Xj

Nonlocal electron kinetics in gas-discharge plasma

L D Tsendin

DOI: 10.3367/UFNe.0180.201002b.0139

Contents

Abstract. The field of electron kinetics in extremely nonequilibrium glow discharge plasma is reviewed, starting from the classical works of Langmuir. It is shown that it is only in terms of kinetics that many aspects of nonequilibrium plasma — such as the structure of near-electrode regions, spatial profiles of ionization and luminosity, striations and particle and energy flows — can be adequately understood.

1. Introduction

The characteristic scales and times of those macroscopic processes that are of the most interest to us usually significantly exceed the lengths and times of interparticle relaxation. Therefore, almost all objects around us can be divided into macroscopically small volumes which are small when compared to macroscopic scales, but considerably exceed the relaxation length. Similarly, the time durations of macroscopic processes we are interested in can usually be divided into macroscopically small time intervals, short in comparison with the macroscopic time, but much longer than the relaxation time. Since the values of these volume parts and time intervals are microscopically large, their state is close to the local thermodynamic equilibrium (LTE). In this case, the state of each part can be characterized by local values of the temperature $T(\mathbf{r}, t)$ and the average mass velocity, pressure, and other macroscopic parameters. Small deviations from the complete thermodynamic equilibrium caused by inhomogeneity and nonstationarity of macroscopic parameters lead to the occurrence of dissipative processes that smooth down these deviations. Such LTE-based media are described within the limits of the hydrodynamic approximation. Then, all local properties of an elementary one-component medium (for example, an ideal gas) can be fully described by five functions of four variables: the density $n(\mathbf{r}, t)$, the three components of the velocity $\mathbf{u}(\mathbf{r}, t)$, and the temperature $T(\mathbf{r}, t)$. The relaxation time in an ideal gas is merely the time τ between collisions, and the relaxation length is the mean free path λ. In essence, the hydrodynamic description represents the description in terms of an 'average Soviet' particle. This particle possesses average directed velocity $\mathbf{u}(\mathbf{r}, t)$ and average chaotic energy $(3/2)\,T(\mathbf{r}, t)$, and in order to obtain the characteristics of the whole ensemble of particles, it is just necessary to multiply them by concentration $n(\mathbf{r}, t)$. The only serious difficulty (in the use of such an approach to phenomena around us) appears when we apply it to processes where solar radiation plays a part. The presence of this radiation, which transfers information about the solar photosphere that is kept at a temperature of 6000 K, makes all phenomena with its participation strongly nonequilibrium. The fact that the concept of temperature makes no sense for systems far from LTE is still unusual for mass awareness.

We cannot say that strongly nonequilibrium systems did not attract the attention of researchers at all; however, throughout the entire 19th century the center of attention was on objects in a state close to LTE that make up mostly our environment. The most impressive advances in thermodynamics, statistical physics, and hydrodynamics achieved at that time were related to the investigation of such systems. To study strongly nonequilibrium systems, it was necessary to abandon a variety of accustomed conceptions and, in essence, to create a new branch of physics, which today is called physical kinetics. Its foundations were laid by J C Maxwell and L Boltzmann.

It was probably a sense of necessity to proceed to a more detailed level of description that led Maxwell to the concept of the velocity distribution function of molecules [1–3]. A

L D Tsendin St. Petersburg State Polytechnical University, ul. Politekhnicheskaya 29, 195251 St. Petersburg, Russian Federation
Tel. (7-812) 534 58 21. E-mail: tsendin@edu.ioffe.ru

Received 16 February 2009, revised 25 April 2009
Uspekhi Fizicheskikh Nauk **180** (2) 139 – 164 (2010)
DOI: 10.3367/UFNr.0180.201002b.0139
Translated by S V Vladimirov; edited by A Radzig

description of many-particle systems in terms of the distribution function is much more detailed than a hydrodynamic description, but it is also a much more difficult one since instead of the five functions of four variables we have to deal with the only one function $f(\mathbf{r}, \mathbf{v}, t)$ which, however, depends on seven arguments: the coordinates, velocities, and time. The kinetic approach is absolutely necessary for describing those phenomena which are determined by a group of particles instead of their whole ensemble, and/or when the distribution function is not of a standard shape (such as Maxwellian). In a sense, the kinetic description differs from the hydrodynamic one in the same way as a free society differs from a totalitarian one: in the hydrodynamic (totalitarian) description, each particle is representative, and the properties of the collective differ from the properties of the individual only by scaling. Whereas the kinetic description is much more flexible and rich, being also more intricate.

Maxwell discovered that in the thermodynamic equilibrium the velocity distribution of molecules of an ideal gas is described by a simple universal relation, which we call the Maxwellian distribution function:

$$f(\mathbf{r}, w, t) = \frac{n(\mathbf{r}, t)}{(2\pi T/m)^{3/2}} \exp\left(-\frac{w}{T(\mathbf{r}, t)}\right), \qquad (1)$$

where $w = mv^2/2$ is the kinetic energy of a molecule, and the temperature is measured in energy units.

The following decisive step was made by Boltzmann [4, 5], who clearly realized that non-Maxwellian distribution functions correspond to nonequilibrium (he called them 'nonstationary') systems, and developed the well-known kinetic equation (now carrying his name) for a nonequilibrium distribution function:

$$\frac{\partial f}{\partial t} + (\mathbf{v}\nabla) f + (\mathbf{F}\nabla_{\mathbf{v}}) f = \sum_{\beta} \mathrm{St}(f, f_{\beta}). \qquad (2)$$

These publications started physical kinetics (see, for example, monograph [6]).

The kinetic analysis is necessary, roughly speaking, in two cases. If LTE takes place, it is necessary to accurately calculate dissipative fluxes and corresponding transport coefficients through parameters of the interactions between particles. However, the kinetic analysis is, of course, absolutely unavoidable for the investigation of systems found far from LTE. A departure from equilibrium for the system can be caused by small characteristic scales of processes of interest to us, in comparison with τ, λ, as well as by the action of external factors.

Among numerous strongly nonequilibrium systems and phenomena, we can single out three basic groups. The first of them includes processes proceeding in dilute gases. Here, for example, is the physics of the interstellar medium penetrated by fluxes of particles (almost noninteracting with themselves) and radiation of various origins.

The second group comprises living matter, including us as well. Here, the nonequilibrium state is supported by the difference between 6000-K solar radiation temperature and the 300 K temperature of our environment.

The third group of strongly nonequilibrium phenomena is related to gas discharges. Of course, this group is of less general interest than the first two but it is significantly simpler. Discharges are quite easy to observe, the means and methods of their diagnostics are well developed, and, importantly, they are relatively cheap. A departure from equilibrium in discharges is created by applying an external voltage to a gas and by releasing Joule heat in the electron subsystem.

The glow discharges created by fields relevant to various frequency ranges exhibit the highest degrees of departure from equilibrium among gas discharges. Glow discharges are characterized by small currents, a low ionization degree, and low pressure (usually significantly smaller than the atmospheric pressure). Because of a huge difference between the electron mass and masses of molecules, relaxation of electron momentum such discharges occurs much faster than that of electron energy, so the energy exchange between electrons and heavy particles is strongly suppressed. The low degree of ionization and low pressure facilitate energy exchange between heavy plasma components (neutral molecules and ions) and the surrounding medium. Therefore, neutral particles, whose number exceeds by many orders of magnitude the number of charged particles, play the role of a heat bath whose temperature usually does not significantly differ from room temperature. At the same time, electron energies are much higher. Since the discharge is sustained, as a rule, by the electron impact ionization of neutral molecules, the characteristic level of the electron energy should be a few electron-volts. Such a medium, called plasma by Langmuir, in each volume of which heavy particles at room temperature co-exist with electrons having energies larger by two orders of magnitude, is, obviously, extremely nonequilibrium and far from LTE. Therefore, the kinetic approach using a particle distribution function (first and foremost that of electrons) as the basic element is absolutely necessary for a plasma analysis. The electron distribution function (EDF) describes electron density in the phase space (the coordinate and velocity space). The EDF is one of the major plasma characteristics; all the parameters of plasma and its existence depend on the EDF properties.

The fact that the investigation of strongly nonequilibrium media is a separate branch of physics was realized relatively late. Apparently, this is because such systems attracted general attention not that long ago, in the 20th century. Therefore, the volume devoted to physical kinetics [6] is the last one in the Landau and Lifshitz course, and the first monograph *The Foundations of Physical Kinetics* by L E Gurevich [7], appeared only in 1940. Furthermore, when Boltzmann formulated the kinetic equation at the beginning of development of physical kinetics, he did not even mention any of the above three groups and pointed out only two possible applications of his equation: ultrasound damping and transport processes in rarefied gases. He wrote, "... In certain transitional cases (very rapid sound waves with evolution of heat, viscosity or heat conduction in very dilute gases) a sharp distinction is no longer possible between visible and thermal motion... . Likewise the gas theory has led to completely new laws in these transition regions which appear to reduce to the usual hydrodynamic equations corrected for viscosity and heat conduction as purely approximate formulae" [5].

It should be emphasized that to date the main results in kinetics have been obtained on the basis of the investigation and solution of the kinetic Boltzmann equation describing an ideal gas, i.e., a system of almost noninteracting particles. This is apparently related to the fact that intensive random interactions lead to establishing LTE. If intensive particle interactions may result in the occurrence of certain order (for

example, crystallization), it is often possible to separate subsystems of weakly interacting quasiparticles, such as phonons in crystals, electrons and holes in semiconductors, and so forth, which are also described by the kinetic Boltzmann equation.

It is necessary to emphasize that the concept of temperature makes sense only in the LTE conditions, and its use in systems found far from equilibrium is, at the very least, irrational. Certainly, it is possible to call temperature 2/3 of the average particle energy and to introduce partial temperatures of various particle groups and sorts, but such a procedure can lead only to a rough approximation which does not have a serious physical foundation. We note, by the way, that the word 'temperature' itself creates an illusion that all-powerful tools of formal thermodynamics can also be applied to strongly nonequilibrium systems, and this is exactly what we should not do. Therefore, it does not seem to be absolutely correct to call the weakly ionized gas-discharge plasma 'low-temperature'. The only exception is the case when, for whatever reasons, the relaxation of particles of some kind among themselves occurs much faster than equilibrium is established between them and other particles. For example, such a situation takes place for the electron subsystem in a plasma (even weakly ionized) in which already at a low degree of ionization the electron–electron collisions establish a Maxwellian electron distribution much faster than the electron energy relaxation in collisions with heavy particles occurs.

Naturally, as a first step Boltzmann applied his new procedure to study systems which reside in a state close to LTE, when deviations of the distribution function from the Maxwellian one are small corrections determining dissipative fluxes. This work was continued by H A Lorentz [8], who calculated the electron mobility by utilizing the Boltzmann equation. In so doing, Lorentz took into account that a small correction to the Maxwellian distribution function is proportional to the cosine of the angle between the electron velocity and the electric field strength. In other words, he used a two-term approximation for the electron distribution function, assuming the isotropic EDF component to be Maxwellian. These or other procedures to calculate small corrections to the Maxwellian distribution function were used by numerous researchers and appeared to be rather effective for describing LTE-systems. The logical conclusion of this course of development was the work by Chapman [9] and Enskog [10], where a procedure was suggested to allow obtaining the complete system of gas hydrodynamic equations and relating the values of dissipative coefficients to the parameters of intermolecular collisions. The previously unknown thermal diffusion phenomenon [9] was thus predicted.

For systems far from LTE, it may be inferred that laboratory plasma where stationary or quasistationary strongly nonequilibrium states can be created without particular problems is the most convenient medium to develop procedures of kinetic analysis for strongly nonequilibrium systems. It is possible to distinguish two major groups of plasma phenomena in which a special, specific role is played by particles belonging to a definite portion of the distribution. First, there are wave–plasma interaction phenomena. Beginning with the classical work by Landau [11], who revealed that Langmuir wave damping is determined by a small group of resonant electrons with velocities close to the wave phase velocity, this area of kinetics has developed quite profoundly and in detail [6, 12, 13]. The second group of kinetic phenomena is related with various plasma-chemical reactions. Since the principle of detailed equilibrium does not take place in strongly nonequilibrium systems [14], and the reaction cross sections strongly depend on the parameters of colliding particles, the reaction rates in strongly nonequilibrium plasma are quite sensitive to the distribution function shape.

Thus, even a stationary composition of plasma is determined not by its temperature (which is absent) but cross sections of particular reactions. Some of these problems were considered in Refs [14–16].

Among plasma-chemical processes, the process of direct impact ionization, which is often the main process that creates plasma, is apparently the simplest and most studied in detail. Since for the plasma to be stationary, for example, the average ionization frequency must be equal to the inverse lifetime of charged particles, being determined by the slow (ion) plasma component, direct ionization is also relatively rare. It is determined, therefore, by a few electrons whose energy significantly exceeds the average value. This portion of the electron distribution function is usually called the tail. Below, we shall concentrate on the basic mechanisms forming EDF tails in glow discharges and on the most obvious macroscopic manifestations of electron kinetics by restricting ourselves to the elementary case of ionization phenomena in atomic gases.

Profound interest in electron kinetics in gas discharges has been characteristic of the physics of gas-discharge plasma since the early stages of its development. The founder of modern plasma physics, Irving Langmuir, showed a profound interest in this problem. The procedure of probe plasma diagnostics originated by Langmuir is to date one of the main sources of information on plasma properties. Almost all information on electron kinetics is obtained by Langmuir probes. Though the EDF shape determines the rates of atomic and molecular excitations and, consequently, in particular, plasma radiation, huge information about the EDF shape, which in principle can be recovered from the optical data, remains to be systematically used for this purpose.

The probe technique gives us a great volume of information on the local and instantaneous values of density and average energy of plasma particles, on the profiles and evolution of plasma electric fields, etc. However, obtaining the quantitative information on the shape of electron distribution appeared to be a bit more difficult.

Despite the fact that Langmuir realized the importance of electron kinetics for understanding plasma phenomena and, in essence, established the experimental technique which is applied up to this day to measure EDF, the results he obtained were quite modest. The first reason is apparently related to the fairly direct approach that he adopted to solve the problems [17]. Langmuir plotted the current–voltage $(C-V)$ characteristics of his probes on a semilogarithmic scale. Thus, it was easy to identify Maxwellian distribution function (1) which corresponded to a straight line, but it was difficult to obtain any quantitative information about non-Maxwellian EDFs. It is necessary to note that there were no known examples of such distribution functions at that time. Therefore, when his semilogarithmic $C-V$ characteristics were deflected from straight lines, Langmuir used the superposition of several Maxwellian EDFs.

It should also be noted that Langmuir used an old ('classical' as he called it) kinetic theory [18, 19] to analyze electron kinetics and, apparently, he was not familiar with the

Boltzmann kinetic equation. Most probably, Langmuir felt the need for a more exact quantitative description of electron kinetics when, for example, he wrote, "...The classical kinetic theory results are useful for easy rough estimates or for use where no more accurate data are available or can be mathematically handled" [17]. However, the kinetic equation was not discussed in his papers, and Boltzmann's name was mentioned only in connection with the Boltzmann relation between the electron number density and the electrostatic potential. It is characteristic of this initial stage of research that in fundamental monographs [20–22] reflecting the state of the ideology for that time, the Boltzmann kinetic equation was not mentioned at all.

The subsequent development of electron kinetics convincingly illustrates the inseparable connection between progress in understanding the physical mechanisms of phenomena and the development of experimental techniques and new theoretical approaches. Systematic measurements and calculations of EDFs in glow discharges began only a few decades later. The first essential steps were taken by M J Druyvesteyn.

First, Druyvesteyn found [23–25] that the second derivative of the probe current I_p with respect to its potential V_p is proportional to the isotropic EDF component $f_0(\mathbf{r}, v, t)$:

$$f_0 \sim \frac{d^2 I_p}{dV_p^2} . \tag{3}$$

Since the relaxation time τ of an electron momentum (the time between collisions) and the corresponding mean free path λ in discharges are usually considerably less than the energy relaxation time τ_ε and length λ_ε, the anisotropy of the EDF is, as a rule, small and the isotropic component f_0 dominates. Therefore, various modifications of the Druyvesteyn method based on Eqn (3) remain up to date at the base of the gas-discharge plasma probe diagnostics serving as the main source of information on electron kinetics.

Druyvesteyn's second remarkable result is the following. By analyzing a spatially homogeneous stationary problem of the EDF shape for a plasma in an electric field, when only elastic electron–atom collisions are essential [23–25], he obtained from the kinetic equation the EDF as

$$f_0(w) \sim \exp\left[-\frac{3m}{M}\left(\frac{w}{eE\lambda}\right)^2\right], \tag{4}$$

where $\lambda = v/\nu$ is the constant transport mean free path, and w is the kinetic energy. That was apparently the first convincing example of an essentially non-Maxwellian EDF. If the mean free path depends on the electron velocity, instead of formula (4) we have

$$f_0(w) \sim \exp\left(-\frac{6m}{Me^2E^2}\int_0^w dw' \, \frac{w'}{\lambda^2(w')}\right). \tag{5}$$

Thus, the Maxwellian EDF (1) is a particular case of expression (5) corresponding to the transport collision frequency not depending on the velocity.

Only at the end of the 1930s, when Langmuir, unfortunately, had already finished his gas-discharge studies, did EDF probe measurements and EDF calculations using the Boltzmann equation become the standard procedure. In their 1940 review [26], Druyvesteyn and Penning wrote, "...The velocity distribution of the electrons is of fundamental importance as in most discharges the current is mainly an electron current and the excitation and ionization of gas atoms is in large part caused by electrons. The calculation of the electron velocity distribution is thus one of the important steps for the understanding of gas discharges."

The fact that the EDF in weak electric fields is usually almost isotropic was used, apparently, for the first time by Lorentz [8], who suggested expanding EDF in $\cos\vartheta$, where ϑ is the angle between the electron velocity and the electric field strength, in order to analyze the electron conductivity of metals. Various modifications of this expansion were subsequently developed in numerous publications [23, 27–31] (see also Refs [32, 33]). It was shown there that in the most important (for gas discharges) conditions of fast electron momentum relaxation this expansion rapidly converges, and in most cases it is sufficient to consider only the scalar and vector components of an EDF expansion in the velocity space. This so-called two-term approximation takes the form

$$f(\mathbf{r}, \mathbf{v}, t) = f_0(\mathbf{r}, v, t) + f_1(\mathbf{r}, v, t)\, Y_1^m(\theta, \varphi) , \tag{6}$$

where Y_1^m are the first spherical harmonics.

Slow electron energy relaxation already leads to significant electron heating by relatively weak fields. Since glow discharges are usually supported by the electron-impact ionization, electron energies should be comparable to the ionization potential, i.e., the EDF energy scale should be on the order of 1 eV. On the other hand, since the degree of ionization in such discharges is extremely small, the neutral gas particles remain almost at room temperature. Therefore, the electron subsystem that creates and supports the discharge is, at the same time, the most nonequilibrium part and demands a kinetic analysis first. The huge (up to two and more orders of magnitude) distinction between the average energies of electrons and heavy particles is the factor characterizing this degree of departure from equilibrium state.

Ionizing electron collisions (without which the discharge does not exist at all) in stationary discharges compensate for relatively slow losses of charged particles. In such collisions, only those electrons which have sufficiently high energy, exceeding the threshold magnitude ε_i, can participate. Ionizing electron collisions occur much less often than collisions of other types, first and foremost elastic collisions. Therefore, the number of such electrons should be relatively small and the threshold energy ε_i should correspond to the EDF tail. Since ionization constitutes one of the inelastic impact types, the most important thing for discharge electron kinetics is to know the correct shape of the EDF tail, whose exponential decrease with energy is determined just by inelastic collisions where a significant part of the electron energy is lost. Therefore, EDFs defined by formulas (4) and (5), calculated without regard for inelastic collisions, are not really suitable for this purpose.

In Refs [20, 34], an investigation began on the influence of collisions with large energy losses on the EDF shape, and expressions were obtained for the 'pipeline' EDF whose formation is determined by the Joule heating and inelastic collisions, whereas small energy losses in elastic collisions are insignificant at all. If energy $eE\lambda$, which an electron acquires (or loses) in an electric field between elastic collisions, is small in comparison with $\varepsilon_1 \sim \varepsilon_i$, then the change of the electron energy represents small random walks. Therefore, Joule heating constitutes diffusion along energy, with the diffusion

coefficient given by

$$D_\varepsilon = \frac{e^2 E^2 \lambda^2 \nu}{3} . \quad (7)$$

In the elementary case, when the transport frequency ν of elastic collisions does not depend on the electron velocity and inelastic collisions with the energy loss $\varepsilon_1 \sim \varepsilon_i$ occur very often (this corresponds to the black or absorbing boundary approximation in diffusion theory), the 'pipeline' EDF, describing electrons which gain energy up to ε_1 and then instantaneously lose it in an inelastic collision, takes the form

$$f(w) \sim \frac{1}{\sqrt{w}} - \frac{1}{\sqrt{\varepsilon_1}} . \quad (8)$$

This EDF is similar to a pipeline where the diffusion along energy delivers electrons with an energy up to the threshold ε_1, and when an electron acquires this energy it immediately undergoes an inelastic collision, loses energy, but again starts to gain it back in the field. These two limiting cases, formulas (5) and (8), correspond to the basic scenarios of EDF formation in stationary or quasistationary glow discharges.

It should be noted that the tails of exponentially decreasing EDFs of the form (5) decrease even more rapidly because of fast electron losses in inelastic impacts. Therefore, the ionization rate, for example, is quite small. It is, roughly speaking, a product of two exponentially small factors: the first one caused by the decrease in the EDF body (5), and the second one by the additional decrease in the EDF tail. Thus, especially in the case of low pressures, in a weak field where the electron energy balance is determined by elastic collisions, and the EDF body by expression (5), it is impossible to compensate for the charged particle losses, yet such compensation is necessary to maintain a stationary discharge. Therefore, as a paradigm for EDF body, at least in the case of discharges in atomic gases at low pressures, it looks more rational to start with expressions like Eqn (8).

The comparatively slow development of the branch of electron kinetics was probably related to the fact that most attention had been focused for a long time on stationary direct current (d.c.) discharges only. To maintain them, the average inverse lifetime of charged particles τ_a^{-1} (in the absence of a magnetic field it is determined by ions) should be equal to the ionization frequency Z averaged over distribution:

$$\tau_a Z = 1 . \quad (9)$$

The time τ_a is stipulated by recombination, which is determined by average electron parameters such as the average gas energy and pressure, and weakly depends on the details of their distributions. For example, in the popular Schottky model for a cylindrical column one finds [35–37]

$$\tau_a = \frac{(R/2.405)^2}{D_{amb}} . \quad (10)$$

This means that the ionization frequency Z is determined by average electron parameters, as well, and detailed knowledge of the EDF tail shape determining Z appears to be excessive in a sense. Using, for example, the expression

$$Z = \sqrt{\frac{4\varepsilon_1}{\pi T}}\, \nu^* \exp\left(-\frac{\varepsilon_1}{T}\right) , \quad (11)$$

for a Maxwellian EDF (1) with $\varepsilon_1 \gg T$ and the ionization frequency ν^* independent of the velocity, it is possible to calculate the electron 'temperature' T. And the energy balance for an electron gas allows obtaining through T the electric field strength maintaining the discharge. On the other hand, according to formulas similar to expression (11) it is possible to obtain values of the level excitation rates, which are of the main interest for the majority of applications. Since EDF tails usually decrease exponentially, replacing T in these expressions by the scale of the EDF tail decrease, namely

$$T^* = \left(\left.\frac{d \ln f}{dw}\right|_{w=\varepsilon_i}\right)^{-1} , \quad (12)$$

usually allows one to take into account the non-Maxwellian character of the EDF tail with an acceptable accuracy. However, relations like (9) do not take place in a nonstationary and nonuniform plasma. Therefore, in such situations, on the contrary, knowledge of the EDF is necessary and taking into account electron kinetics leads to a number of nontrivial phenomena.

2. Microwave breakdown

During WWII, electron kinetics was developed along two main lines. The results of this work are summarized in numerous articles and reviews that were published in the following years. The first line was related to microwave breakdown of gas-filled gaps [38–43], and the second one to the problems pertaining to nonlinear electrodynamics, which appear in the propagation of high-power radio waves [44, 45].

The kinetic equation analysis in these cases was based on the faster momentum (than the energy) relaxation:

$$\tau, \lambda \ll \tau_\varepsilon, \lambda_\varepsilon . \quad (13)$$

For example, in atomic gases in the conditions when the main energy is lost in elastic collisions, the ratio between two relaxation times is $\tau/\tau_\varepsilon = \delta = 2m/M \sim 10^{-4}$ for an EDF body (i.e., for electrons with energies below the first excitation potential ε_1). The ratio between appropriate relaxation lengths (which is a square root of this quantity) is small, too. Therefore, the analysis of the kinetic equation in the above-cited works (see also Ref. [46]) was based on two-term approximation (6). If the field frequency satisfies the inequality $\omega\tau_\varepsilon \gg 1$, the main (isotropic) EDF component f_0 cannot follow it and is stationary.

In a sinusoidal field $E_0 \sin \omega t$, expressions for the ionization and excitation rates coincide with the respective expressions for a constant field after replacement of its strength by the effective value $E_0/\sqrt{2}$. In the case of a quasistationary field, $\omega\tau_\varepsilon \ll 1$, the EDF at each instant of time is given by the same expressions for a constant field, but now it is determined by the instantaneous field strength $E(t)$. Since the energy relaxation for the EDF tail occurs much faster than that for small energies, such classification of the frequency ranges turns to be too rough. The energy relaxation time τ_ε for the EDF tail is significantly smaller than τ/δ and almost coincides with the inelastic collision time τ^*, which is only 10–100 times more than the momentum relaxation time τ, meaning that within a considerable range of frequencies the EDF body is determined by the effective electric field, and its tail by the instantaneous field [47].

In a nonuniform plasma, the same classification is valid for spatial scales. The energy relaxation length for the EDF

tail is $\lambda^* = \lambda\sqrt{\tau^*/\tau}$, whereas for the EDF body it is much longer: $\lambda_\varepsilon = \lambda/\sqrt{\delta} \gg \lambda^*$. If the problem scale satisfies the inequalities

$$R \gg \lambda_\varepsilon \gg \lambda^*, \tag{14}$$

then the traditional local approximation can be applied: the EDF shape is determined by a local heating field according to the same formulas as in a uniform plasma. Thus, the EDF can be represented as a product of the electron concentration $n(\mathbf{r}, t)$ and a velocity function normalized to unity. The space and time dependences of this function are expressed only through the strength of the field heating electrons and other external parameters. We also note that in this case the ambipolar (i.e., transverse to the current flow) electric field is usually weak and the heating field coincides with the total field.

If inequality (14) is not fulfilled, nonlocal effects become essential in the EDF formation. Bernstein and Holstein [48] demonstrated that the kinetic equation for $f_0(r, v)$ in the positive column (PC) of a direct current discharge can be reduced to an equation of two-dimensional diffusion along the radius r and by the total energy $\varepsilon = e\varphi(r) + mv^2/2$, where $\varphi(r)$ is the radial electrostatic potential. If the tube radius R exceeds both the energy relaxation lengths, λ_ε and λ^*, then for a radial displacement of an electron its total energy ε is conserved, so that the EDF f_0 becomes fully nonlocal. For electrons locked in the radial potential well $\varphi(r)$, the EDF depends only on ε. The kinetic equation for $f_0(\varepsilon)$ can thus be averaged over the part of the tube section, which can be accessed by an electron with the total energy ε.

Therefore, the radial plasma inhomogeneity and the radial electric field do not enter explicitly in the averaged kinetic equation for $f_0(r, v)$ and it can formally be reduced to the equation for a uniform plasma in a uniform field. The only essential difference lies in the fact that in a fully nonlocal case the EDF depends on the total energy ε instead of the electron kinetic energy $w = mv^2/2$.

Despite the fact that a significant (if not the main) part of EDF probe measurements was done just in this fully nonlocal mode (14), the fundamental work [48] was completely forgotten, so that the nonlocality of the EDF was rediscovered twenty years later [49]. In Refs [50, 51], an analysis of the PC was done and it was shown that in the transit-time regime,

$$\lambda \gg R, \tag{15}$$

the EDF anisotropy also remains small and most of it depends only on the total energy, but the traditional expansion in spherical harmonics, which is the basis of the two-term approximation (6), needs to be modified. If the total electron energy exceeds the wall potential, the electrons moving almost perpendicular to the wall quickly move to it, so the EDF angular dependence in the velocity space becomes discontinuous. Therefore, amplitudes of all spherical harmonics (except the zero one) are comparable and a power series in them converges poorly.

The fact that at low pressures the second derivative of the probe current with respect to its potential (3) does not depend on the probe position, thus pointing to nonlocal EDF $f_0(\varepsilon)$ and its independence from coordinates, was apparently observed repeatedly but did not attract special attention. Such an experiment is exemplified in Fig. 1.

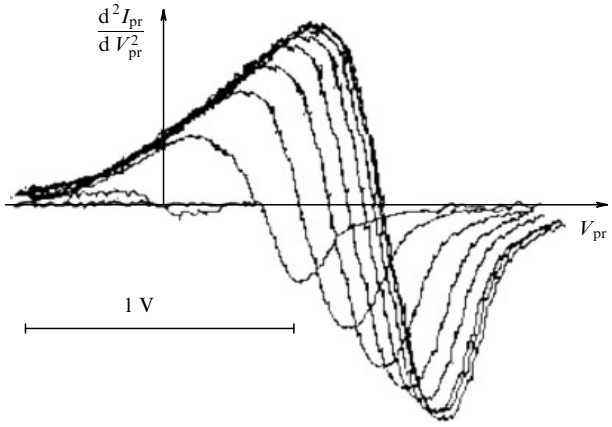

Figure 1. The second derivatives of the probe current at different points of a discharge gap [52]. The discharge is set up in Xe at 0.1 Torr and $I = 2$ mA. Matching of the left parts of the curves indicates that the EDF depends only on the total energy ε.

Another phenomenon for which the usual two-term description of the EDF appears to be insufficient is the well-known runaway effect for electrons. Since the Rutherford cross section for electron scattering on Coulomb potential quickly ($\sim w^{-2}$) decreases with increasing energy, then if an electric field is applied to a fully ionized plasma, the plasma becomes more and more transparent for accelerating electrons and a finite probability appears that an electron will turn to a run-away electron. This effect, discovered by Dreicer [53, 54], and the relevant analytical solution [55] (see also Ref. [56]) surprised the plasma community.

Since all electron–atom cross sections at large energies are asymptotically Rutherford ones, this effect takes place in a weakly ionized plasma, as well. The main difference resides in that the runaway process proceeding with fast electrons in a neutral gas is accompanied by the continuous production of slow electrons [57]. In sufficiently strong fields, slow electrons can also run away, so that the number of runaway electrons can increase in time exponentially. The dynamic friction force (Bethe–Bloch force) acting on fast electrons decreases with increasing energy as $\sim w^{-1}$. However, it is approximately constant for small energies.

In Refs [58, 59], a simple model was considered, where the scattering was not taken into account. For energies smaller than w_0, the friction force is constant, and for larger energies it obeys the Bethe–Bloch law. Then, it appeared that if the field strength exceeds the maximum of the retarding force, an exponential increase in the number of run-away electrons takes place and their multiplication time grows exponentially with the field strengthening.

For relativistic energies, the retarding force becomes an increasing function of w. It was pointed out in Ref. [60] that an exponential multiplication of relativistic run-away electrons can take place in this case. The time and length of this multiplication turn out to be quite large. Indeed, for normal conditions the multiplication length makes up a few dozen or hundreds of meters. This effect plays an important role for some atmospheric phenomena [60].

In all the above-cited publications, the only physical mechanism considered, which transformed energy gained by electrons in a field into thermal energy, was that involving collisions with heavy particles (neutrals). On the other hand, away back in 1925 Langmuir pointed out [61] that electron collisions with chaotic oscillating electric fields can play the

same role. In particular, he suggested that such oscillations can 'Maxwellize' the EDF, which would explain the fact that EDFs observed by him at small pressures are rather close to Maxwellian distributions functions. This phenomenon was called the Langmuir paradox by Gabor et al. [62]. However, searches for such oscillations have not yet given a convincing result. Besides, it is hardly likely that electron interactions with oscillations should invariably form a Maxwellian EDF. Thus, this question requires careful investigation and still remains open [63].

Godyak [64, 65] noticed that even interaction of electrons with regular electric fields in sheaths of radio-frequency discharge strongly affects the EDF and can lead to collisionless electron heating [12]. The current state of the problem of so-called stochastic electron heating is discussed in detail, for instance, in Refs [66–68].

3. Probe diagnostics and measuring the electron distribution function (EDF)

For the first several decades, most studies into discharges were carried out at the phenomenological level. The results of direct optical measurements and the electrical characteristics of discharge as a whole were all that was available. Therefore, to date a direct current glow discharge, for example, is traditionally divided according to its glow into a cathode dark space, a negative glow, a Faraday dark space, and a positive column.

However, the radiation emitted by a discharge is a result of a complex chain of electrodynamic, kinetic, and transport processes and it is not related directly to such 'manually' set external parameters as the discharge tube and electrode geometries, the gas composition and pressure, the current, or the deposited power. It was impossible to track this chain and to clarify the physical mechanisms of these relations in the absence of information on discharge plasma parameters. At the same time, experimental investigations of internal characteristics were faced with a basic problem that plasma perturbations introduced by any measuring device placed inside cannot be made small. Therefore, the decisive step made by Langmuir was that since we cannot make the perturbation small, we need to include the perturbed region in the device ideologically. In other words, it is necessary to know precisely what occurs in the perturbed region in order to be able to relate exactly and unambiguously the unperturbed plasma parameters to the readings of instruments consisting of iron and glass pieces. If the probe size and the plasma region which it perturbs are small, so that the plasma can be considered undisturbed far from this region, then electrons coming to the probe bring information on the unperturbed plasma, and only the recalculation algorithm should be found in order to recover this information from the known probe signal.

The first information about internal discharge properties was that the main part of the voltage applied to the discharge is screened in the volume charge sheaths (layers). The field there is strong, whereas the main part of the discharge is occupied by a quasineutral plasma where the field is weaker than in the sheaths by orders of magnitude [17].

The plasma–sheath boundary should not coincide at all and does not coincide with any one of the visually observable boundaries. In the cathode sheath of a direct current discharge, for example, the electron flux and consequently the glow exponentially increase with distance from the cathode. Therefore, part of the sheath is dark. The glow intensity, which, roughly speaking, is proportional to the concentration of fast electrons accelerated by the strong plasma sheath field, exponentially increases with distance from the cathode. On the other hand, the number of fast electrons in the plasma decreases with distance. Therefore, the negative glow (from which the glow discharge obtained its name) already begins in the volume charge sheath at a distance on the order of the ionization length from the plasma boundary, and the *maximum* glow corresponds to the plasma–sheath boundary.

Fast electrons accelerated by the strong sheath field penetrate into the plasma where the field is almost absent and cause nonlocal ionization and radiation emission in the plasma part of the negative glow region. In the region where the electrons' path finishes and their energy is depleted, there is a boundary between the negative glow and the Faraday dark space. Identifying the cathode sheath with the cathode dark space sometimes still occurs, as does the negative glow with the plasma, being one of the difficulties preventing the development of a consistent view of processes proceeding in this important discharge region.

Langmuir clearly realized that probe diagnostics allow obtaining information on important discharge characteristics, such as the EDF. He wrote, "... As the collector is made more negative, the lower speed electrons fail to reach the collector, although those with high speed may still reach it. The volt–ampere characteristic of a collector therefore gives indications as to the distribution of velocities among the electrons in the ionized gas" [17].

Since most of Langmuir's experiments were conducted with relatively high currents, for which the degree of plasma ionization is of the order of 1% or even higher, the interelectron collisions occurred sufficiently frequent, and therefore the EDF body (i.e. a portion of the curve corresponding to electron energies below the first excitation potential of neutrals) was close to the Maxwellian distribution. Thus, essential deviations could be expected only on the EDF tail, where the accuracy of probe measurements is much lower. Therefore, the majority of $C-V$ characteristics obtained by Langmuir were straight lines on the semilogarithmic scale: "The semilogarithmic plots... were in most cases satisfactorily straight over a range covering a 1000-fold increase in the probe current. A few of the curves, however, showed considerable deflections from straight lines, which were greater than the probable errors in the measurements; and these probably indicated deviations from a Maxwellian distribution of velocities... . The broken line [bi-Maxwellian approximation of EDF, for which the upper portion of the $C-V$ characteristic corresponded to low-energy electrons — L.D.T.] gave $T_e = 23{,}000$ K for the lower portion, and 30,200 K for the upper portion... . Deviations of this character, however, seemed to bear no definite relation to the known variables and are therefore probably to be looked upon as a type of experimental error due to some uncontrolled factor" [17].

Systematic EDF probe measurements, however, began a few decades later once Druyvesteyn [23–25] has been obtained relation (3). Since the momentum relaxation time (the time between collisions) τ and the corresponding mean free path λ in discharges are usually considerably less than the energy relaxation time τ_ε and the energy relaxation length λ_ε, the EDF anisotropy is also small, and Eqn (3) determines the main, isotropic, EDF component. Thus, various modifica-

tions of formula (3) dominate in EDF probe diagnostics even up to this day.

The further development of plasma kinetics was strongly influenced by the radio engineering methods which started to be developed by Boyd and colleagues [69–72]. These methods allowed significantly simplifying the technique and increasing its accuracy, so that the EDF probe measurement is currently one of the standard diagnostics of a low-temperature plasma. In particular, it turned out that the EDF in glow discharges (in low-current, low-pressure discharges) is almost never a Maxwellian one. It was especially essential that there was a tail depletion of observed EDFs compared to Maxwellian distributions with the same average energy. EDFs appeared to be surprisingly composite and nonmonotonic in striations, especially at small currents.

With Langmuir probes, a huge amount of detailed information was gathered on the concentration profiles, average energy of electrons, and field distributions in plasmas. Most of the data on electron kinetics was also obtained by probe methods. The history of its advancement convincingly demonstrates the close connection between the progress in understanding the physical nature of phenomena and the development of experimental methods and new theoretical approaches.

Initial application of probe methods was restricted to direct current discharges. The nonlinearity of a radio-frequency sheath led to uncontrollable distortions of the probe's $C-V$ characteristics, impeding their employment. These difficulties were overcome in Refs [73, 74], which allowed applying the Druyvesteyn method to EDF measurements in these discharges, as well.

In essence, the main idea of the EDF probe diagnostics and of the above-mentioned EDF nonlocality lies in the fact that, according to Liouvilles theorem, the EDF is a function of integrals of motion. Thus, if the size of the probe (and that of the region perturbed by it) is small in comparison with λ, the EDF of electrons coming to the probe, expressed as a function of integrals of motion, coincides with the EDF in the unperturbed plasma. In the simplest case when the unperturbed EDF is isotropic, the method of its restoration is given by the Druyvesteyn formula (3). Then, the EDF in the near-probe region depends only on the total electron energy (the kinetic energy plus the potential energy in the probe field) and is not coordinate-dependent. More accurately, it depends on the coordinate as a parameter only. If the unperturbed EDF is anisotropic, then it is possible to obtain the information on anisotropy by varying probe parameters. For example, if the EDF depends on one angle in the velocity space, then by changing the orientation of a plane probe one can recover this dependence [75, 76].

An essential restriction on the applicability of Langmuir probes in the conditions of high pressures resides in that their sizes should be small in comparison with λ. However, the EDF in discharge plasmas is usually close to an isotropic function and its relaxation length is not λ but λ_ε, λ^*, and electrons carry information to the probe from such a distance. Therefore, information on EDFs (in the unperturbed plasma, of course) can also be obtained with much larger probes, with the size limited by the energy relaxation length λ_ε, λ^* [75, 78].

When all discharge volume is less than λ_ε and the EDF is isotropic, the only integral of motion is the total energy ε (the kinetic energy plus the potential energy in the total field), so that the EDF depends only on ε in the whole discharge volume.

Extensive probe investigations of EDFs in our country were launched and developed by Yu M Kagan and V I Perel' [79, 80].

In recent decades, the electron kinetics of glow discharges has developed into a very wide field of science. Therefore, the text below is not claimed to be complete and reflects the interests and opinions of the author.

4. Electron distribution function in a nonuniform plasma. Nonlocality of EDF

When both a plasma and an electric field are uniform, the EDF depends only on electron velocity. This situation was analyzed in numerous publications. Now, the procedure for solving the one-dimensional Boltzmann equation, given the sufficiently detailed databank on cross sections of elementary processes, faces no serious difficulties [81, 82]. However, real plasma is always a nonuniform and nonstationary medium. The simplest case corresponds to the so-called local approximation, when the isotropic part of the EDF is given by the same expressions as Eqns (5) and (8), with the field strengths and concentrations depending on coordinates and time. The directional part of the EDF takes thus the form

$$\mathbf{f}_1 = -\frac{v}{\nu}\,\nabla f_0 - \frac{e\mathbf{E}}{m\nu}\,\frac{\partial f_0}{\partial v}\,.$$

In a uniform electric field, this expression corresponds to an isotropic diffusive spreading of an electron bunch drifting with a constant drift velocity. It was a big surprise when in electron swarm experiments the fact was discovered that this bunch is not a ball, as expected, but an ellipsoid of revolution extended or oblate along the field direction, depending on the sort of gas [83, 84]. The reason of this phenomenon has to do with the following [83–86]. For the EDF to come to equilibrium with a field, it is necessary that after formation of an electron swarm, time t significantly exceeding $(m\nu/M)^{-1}$ has passed. Then, the swarm will drift across the field over a distance $L \sim eE/(m\bar{\nu})$ considerably exceeding the length of its diffuse spreading, $R \sim \sqrt{t\bar{\varepsilon}/(m\bar{\nu})}$, which is much more than the energy relaxation length λ_ε. Here, $\bar{\nu}$ and $\bar{\varepsilon}$ are the values of the transport collision frequency and electron energy averaged over the EDF. In this case, electrons in the front part of the swarm are 'hotter' by a magnitude on the order of λ_ε/R than when they are in the back part. Hence, the drift velocity of the front part of the electron swarm differs from the drift velocity of its back part by a magnitude on the order of λ_ε/R. The drift displacements of the front and back parts of the swarm will also differ by $\sim L\lambda_\varepsilon/R \sim R$.

Thus, if the electron–atom collision frequency increases with increasing electron energy, the drift velocity of the front part of the swarm will be less than that of the back part, and the swarm will acquire the shape of an oblate ellipsoid of revolution. Otherwise, the swarm will be extended along the field direction. An observer perceives these phenomena as anisotropic diffusion. When the inhomogeneity scale is comparable to λ_ε or small in comparison with λ_ε, manifestations of EDF nonlocality are much more diverse.

One of the most characteristic properties of low-pressure discharges is that they are surprisingly quiet and homogeneous. Contrary to high-pressure discharges, they are free from various constrictions (constriction is the major factor complicating numerous practical applications). The reason is that in the local approximation, which is valid at high pressures, the EDF tail and, consequently, the ionization

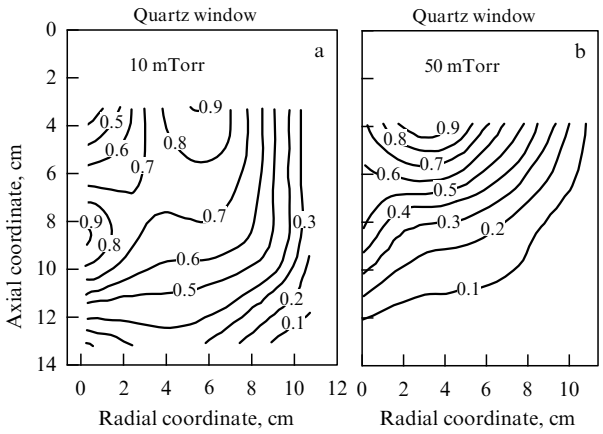

Figure 2. Lines of constant brightness of an inductive radio-frequency discharge in Ar for various pressures [87, 88]. The pancake coil which served for the radio-frequency power deposition to the discharge was installed over the quartz window on the end of the cylindrical discharge vessel. Displacement of the maximum of discharge glow from the vicinity of the coil to the vessel center is clearly seen as the pressure decreases.

rate are rigidly bound to a local electric field which heats up the electrons. This being so, any process strengthening the field in plasma constrictions and thereby the ionization rate in them leads to ionization instability. As a result of its development, sharply nonuniform plasma density profiles are formed.

The nonuniform Joule heating of neutral gas and Maxwellization of the EDF tail caused by interelectron collisions are indicated as the main instability mechanisms. In low-pressure discharges, due to the EDF nonlocality, the ionization rate profile and, consequently, the concentration profile are bell-shaped, independent of the spatial distribution and the energy deposition mechanism.

Indeed, since a nonlocal EDF depends only on the total energy ε, the ambipolar field leads to the maximum of plasma generation near the maximum of the ambipolar potential. An electron with total energy ε also executes motion around the same maximum, and here are the maximum of the ionization rate and the maximum of plasma density, as well. Assuming that this point coincides with the geometrical center of discharge, we obtain a closed consistent pattern. Results of numerical calculations and experiments agree with it well. An example of how the plasma density maximum moves from the region of the maximum energy deposition to the discharge geometrical center is given in Fig. 2.

Introducing the total energy $\varepsilon = mv^2/2 - e\varphi$ and decomposing the electric field into the quasistationary ambipolar component $-\nabla\varphi(\mathbf{r}, t)$ and the radio-frequency field which we consider monochromatic, $\tilde{\mathbf{E}} = \mathbf{E}_{0\omega} \exp(-i\omega t)$, we arrive at a simple equation for the EDF vector component $\mathbf{f}_1(\mathbf{r}, \varepsilon, t)$ in two-term approximation (6):

$$-i\omega\mathbf{f}_1 + v\nabla_\varepsilon f_0 - e\tilde{\mathbf{E}}\,\frac{\partial f_0}{\partial\varepsilon} + \nu\mathbf{f}_1 = 0\,, \tag{16}$$

where the gradient is calculated at the fixed ε. As concerns the isotropic EDF component, $f_0(\mathbf{r}, v, t)$, its shape has no time to trace the field change if the frequency ω of the radio-frequency field $\tilde{\mathbf{E}}(\mathbf{r}, t)$ maintaining the discharge exceeds the energy relaxation frequency: $\omega \gg \max(\tau_\varepsilon^{-1}, \tau^{*-1})$; therefore, the equation for $f_0(\mathbf{r}, v, t)$ can be averaged over fast field oscillations. Substituting expression (16) for $\mathbf{f}_1$ in Eqn (2), using the standard expression for the isotropic harmonic of the collision integral [6, 46], and averaging quantities over time, we obtain the equation for f_0 in the form

$$\begin{aligned} -\frac{\partial f_0}{\partial t} + \frac{1}{v}\left(\nabla_\varepsilon\, vD(w)\nabla_\varepsilon\right) f_0 \\ + \frac{1}{v}\,\frac{\partial}{\partial\varepsilon}\left[v\left(D_\varepsilon(\mathbf{r}, w, t)\,\frac{\partial f_0}{\partial\varepsilon} + V_\varepsilon(w) f_0\right)\right] \\ = \mathrm{St}^{\mathrm{inel}}(f_0) = Nv\sum_k\left[\sigma_k(w)\, f_0(\mathbf{r}, \varepsilon, t)\right. \\ \left. - \sqrt{1 + \frac{\varepsilon_k}{w}}\,\sigma(w + \varepsilon_k)\, f_0(\mathbf{r}, \varepsilon + \varepsilon_k, t)\right], \end{aligned} \tag{17}$$

where $\sigma_k(w) = \nu_k^*(w)/(Nv)$ is the excitation cross section for the kth level, D_ε is the energy diffusion coefficient, and the spatial diffusion coefficient is given by

$$\begin{aligned} D &= \frac{v^2\nu}{3}\,, \\ V_\varepsilon &= \frac{2m}{M}\,\nu w\,. \end{aligned} \tag{18}$$

For a monochromatic field with the amplitude $E_{0\omega}$, we have, for example, the following expression for the energy diffusion coefficient:

$$D_\varepsilon = \frac{e^2 E_{0\omega}^2 v^2 \nu}{6(\omega^2 + \nu^2)}\,. \tag{19}$$

As a result, the Boltzmann equation reduces to a simple equation of diffusion occuring in total energy and in space. The energy flux along the axis is given by

$$\Gamma_\varepsilon = -\left(D_\varepsilon(\mathbf{r}, w, t)\,\frac{\partial f_0}{\partial\varepsilon} + V_\varepsilon(w) f_0\right), \tag{20}$$

while the differential spatial flux (the flux density of electrons with the energy ε per unit energy interval) is defined as

$$\mathbf{\Phi}(\varepsilon, \mathbf{r}) = -\frac{v^3}{\nu(v)}\,\nabla_\varepsilon f_0(\varepsilon, \mathbf{r})\,. \tag{21}$$

In low-pressure discharges, elastic electron collisions [the second term on the right-hand side of expression (20)] usually lead to a small contribution to the energy balance. Therefore, for simplicity, below we omit this term in equation (17). Expression (19) for the energy diffusion coefficient D_ε has a simple evident interpretation. Since the EDF is almost isotropic, the directional velocity $\Delta\mathbf{v}$ is small in comparison with the chaotic velocity. It follows the equation

$$m\,\frac{\mathrm{d}\Delta\mathbf{v}}{\mathrm{d}t} = e\mathbf{E}_0 \exp(-i\omega t) - m\nu\,\Delta\mathbf{v}\,.$$

In collisions, the directional velocity transforms into the random velocity. In other words, each collision is equivalent to a randomly directed velocity vector step on the order of $\Delta\mathbf{v} = e\mathbf{E}_{0\omega}/[m(\nu - i\omega)]$. In this case, the energy step

$$\Delta\varepsilon = mv\,\Delta v\cos\theta\,,$$

where θ is the scattering angle. Thus, Eqn (19) represents a standard expression for the diffusion coefficient, equal to the

product of the square of an average step of random walks (in energy) and the frequency ν of these steps:

$$D_\varepsilon = \left\langle (\Delta\varepsilon)^2 \nu \right\rangle = \frac{e^2 E_{0\omega}^2 v^2 \nu}{6(\omega^2 + \nu^2)} , \tag{22}$$

where the factor $1/6$ appears as a result of averaging over high-frequency oscillations and over $\cos^2\theta$.

In a spatially homogeneous plasma, interpretation of equation (17) as a condition for maintaining the energy flux Γ_e was suggested by Allis and Haus [89]. The convenience of this interpretation becomes especially obvious in an inhomogeneous plasma (see, for example, Refs [90, 91]).

5. Positive column of a direct current discharge

The PC of a direct-current glow discharge is, perhaps, the most studied gas-discharge object. Its stability, the simplicity of its realization and diagnostics, as well as the comparative cheapness of experiments (which is also important), make it the most convenient object for investigation of kinetic phenomena. When analyzing the macroscopic effects of EDF nonlocality, it is simpler to include only the radial potential $\varphi(r)$ in the total energy, and to define the energy diffusion coefficient as

$$D_\varepsilon = \frac{(\Delta\varepsilon)^2 \nu}{3} = \frac{e^2 E^2 \lambda^2 \nu}{3} , \tag{23}$$

where E is the uniform longitudinal field strength, and λ is the mean free path.

The standard local hydrodynamic approximation is valid if the following inequalities hold true:

$$R \gg \lambda_\varepsilon \gg \lambda^* . \tag{24}$$

In this case, the isotropic EDF component can be factorized:

$$f_0(r, w) = n(r)\, F\left(w, \frac{E}{p}\right) , \tag{25}$$

where the function $F(w, E/p)$ is normalized to unity and depends only on the local value of E/p.

If the PC radius satisfies a reverse inequality, namely

$$R \ll \lambda^* \ll \lambda_\varepsilon , \tag{26}$$

then the isotropic EDF component of electrons trapped in the ambipolar field only depends on the total energy, $f_0(\varepsilon)$, whereas small corrections to it, depending on the radius, are responsible for the formation of differential spatial fluxes (21). As an electron moves much faster than the change in its energy takes place, these fluxes for different values of ε are independent of each other and can even be oppositely directed [90, 92, 93].

In equation (17), the radial terms are the most important; they can be eliminated by averaging over the region accessible to an electron with energy ε, so that Eqn (21) is reduced to a one-dimensional equation. The surprising effect is that in the limiting case of a local EDF, as well as in this completely opposite nonlocal limiting case, the forms of the kinetic equation are identical; the only difference consists in the replacement of kinetic energy w in the local case by the total energy ε in the nonlocal case.

Thus, the following contentions are true in a completely nonlocal case (26):

(1) The electron kinetics are completely described by one function of the total electron energy.

(2) Irrespective of the number of spatial coordinates, this function of the total energy is determined by a one-dimensional averaged ordinary differential equation.

(3) The EDF of the kinetic energy can be retrieved at any point from $f_0(\varepsilon)$ by the 'generalized Boltzmann relation' [92, 93].

The averaging procedure for the quantity G is determined according to the relationship

$$\overline{G}(\varepsilon) = \frac{1}{V_0} \int_{V_{ac}} G(\varepsilon, r)\, \mathrm{d}V . \tag{27}$$

Here, V_0 is the full discharge volume, and the accessible volume V_{ac} is set by the inequality

$$\varepsilon \geqslant -e\varphi(r) . \tag{28}$$

The boundary of the accessible volume V_{ac} in formula (27) satisfies the equality $w(S_{ac}) = 0$. If the energy losses in elastic collisions are neglected, the equation for trapped electrons (17) is reduced to the following:

$$-\frac{\mathrm{d}}{\mathrm{d}\varepsilon} \overline{w^{1/2} \left(D_\varepsilon(\varepsilon)\, \frac{\mathrm{d}f_0^{(0)}(\varepsilon)}{\mathrm{d}\varepsilon} \right)} = \overline{w^{1/2}\, \mathrm{St}^{\mathrm{inel}}(w)}\, f_0^{(0)}(\varepsilon) . \tag{29}$$

Here, the notation is used:

$$\begin{aligned} \overline{w^{1/2}\, \mathrm{St}^{\mathrm{inel}}(w)}\, f_0^{(0)}(\varepsilon) &= -\sum_k \Big[\overline{w^{1/2} \nu_k^*(w)}\, f_0^{(0)}(\varepsilon) \\ &\quad - \overline{w^{1/2} \nu_k^*(w + \varepsilon_k)}\, f_0^{(0)}(\varepsilon + \varepsilon_k) \Big] , \\ \overline{w^{1/2} \nu_k^*(w)} &= \frac{1}{V_0} \int_{w(r) \geqslant \varepsilon_k} w^{1/2}(r)\, \nu_k^*\big[w(r)\big]\, \mathrm{d}V . \end{aligned} \tag{30}$$

The last averaging is carried out over the excitation region satisfying the condition $w > \varepsilon_k$, where collisions are accompanied by excitation of the kth level (Fig. 3).

It is necessary to stress that averaging procedures defined by formulas (27), (30) and applied to kinetic equation (17) is just a mathematical reflection of the physical fact that spatial diffusion occurs much faster than diffusion along energy. Thus, the energy acquired by an electron from the heating field is redistributed in the whole volume accessible to it; hence, all this volume participates in the formation of EDF $f_0(\varepsilon)$. The averaging procedure is not related to information loss, so that this EDF in combination with the radial potential profile contains the full information about the EDF in the whole volume. The 'generalized Boltzmann relation', which can be used to restore the EDF of the kinetic energy on the basis of known functions $f_0(\varepsilon)$ and $\varphi(r)$, is given by

$$f_0(w, r) = f_0^{(0)}\big[\varepsilon = w - e\varphi(r)\big] . \tag{31}$$

The restoration procedure is illustrated in Fig. 3.

The pipeline EDF (8), which corresponds to the Joule heating delivering electrons without losses of energy in elastic collisions into the EDF tail where they experience inelastic collisions, takes a simple form in the absorbing boundary

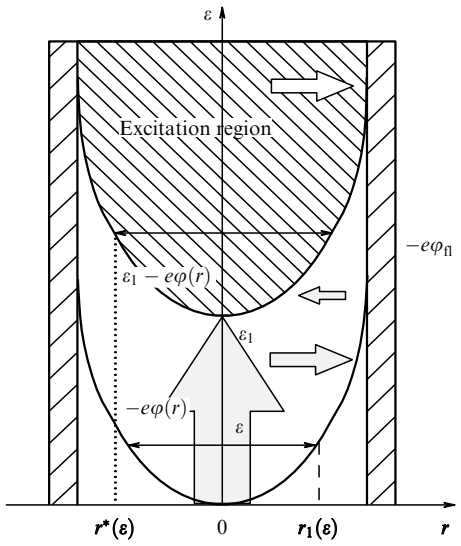

Figure 3. The plane (ε, r) for trapped electrons. The volume accessible to electrons is restricted by the requirement $\varepsilon \geqslant -e\varphi(r)$. In the shaded region of excitation, $r < r^*(\varepsilon)$, the electron energy $w > \varepsilon_1$, and they are able to excite neutral particles. The position of the turning point $r_1(\varepsilon)$ satisfies the condition $\varepsilon = -e\varphi(r_1)$. The vertical arrow corresponds to the energy flux Γ_ε (20) caused by Joule heating, and the horizontal arrows correspond to the differential spatial fluxes Φ (21).

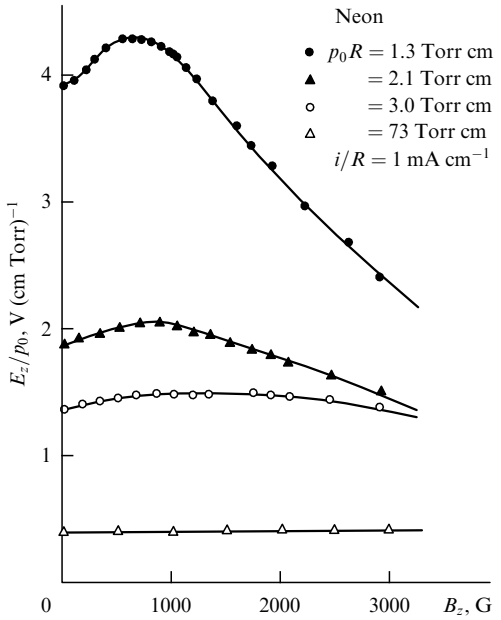

Figure 4. Dependences $E_z(B_z)$ in Ne for $i/R = 1$ mA cm^{-1} and various p_0R [94].

approximation $(v^*(\varepsilon) \to \infty)$:

$$f_0^{(0)}(\varepsilon) = \int_\varepsilon^{\varepsilon_1} \frac{\mathrm{d}\varepsilon'}{w^{1/2} D_\varepsilon(\varepsilon')} \,. \tag{32}$$

For a nonlocal EDF, the boundary between the EDF body and tail, where its fast decrease begins, corresponds to $\varepsilon = \varepsilon_1$ (see Fig. 3), in contrast to $w = \varepsilon_1$ in the local case.

At first glance it seems to be paradoxical that a nonlocal EDF on the periphery shows a decrease because of inelastic collisions in that region of the phase space where these events do not occur, namely, for $w < \varepsilon_1$, and $\varepsilon > \varepsilon_1$. The reason is that at these values of ε, inelastic collisions take place in the discharge center, whereas the differential spatial flux caused by a small addition to the EDF, $f_0^{(1)}(\varepsilon, r)$, delivers particles from the periphery to the center where the inelastic collisions take place. Though the correction $f_0^{(1)}$ is small, the divergence of the differential fluxes caused by it is considerable. It should be noted that the size of the region accessible to an electron with energy ε widens with increasing ε. Therefore, the differential radial flux is directed outward for $\varepsilon < \varepsilon_1$. On the other hand, electrons with energy $\varepsilon > e\varphi_{fl}$ leave to the vessel wall, whose floating potential is equal to φ_{fl}. This means that the differential flux of these electrons is also directed outward at the periphery.

This complex pattern, where different groups of electrons behave almost independently, does not fit in any way into the Procrustean bed of any modification of the hydrodynamic approach operating with characteristics of an 'average Soviet electron'. In our example, this approximation results in a small radial flux on the order of $n_e D_{amb}/R$, where D_{amb} is the ambipolar diffusion coefficient. It is easy to see from Fig. 3 that this small flux is a result of almost complete compensation of much more considerable oppositely directed differential fluxes which are transported by electrons belonging to different parts of the EDF.

Attempts to describe hydrodynamically the electron energy flux lead to similar paradoxes. Since the ambipolar electron flux is very small, the energy flux is related only to the electron thermal conductivity in the hydrodynamic approximation. The profile of the 'electron temperature' $T_e(x)$ is determined by the EDF body, where $\varepsilon < \varepsilon_1$. Consequently, the gradient of $T_e(x)$, determining the thermal conductivity flux, depends on the functions $v(w)$ as well as on the radial profile of the potential $\varphi(r)$. Therefore, the physically absurd possibility of a thermal flux directed towards the 'temperature' increase cannot be excluded.

For the electron density, we have

$$n_e(r) = \frac{4\pi\sqrt{2}}{m^{3/2}} \int_{-e\varphi(r)}^{\infty} \sqrt{\varepsilon + e\varphi(r)}\, f_0(\varepsilon)\, \mathrm{d}\varepsilon \,. \tag{33}$$

In the case of a Maxwellian EDF, expression (33) goes over into the Boltzmann relation.

The fact that the nonlocal EDF $f_0(\varepsilon)$ depends only on the total energy extremely simplifies numerical modeling. Irrespective of the number of space dimensions, the EDF is defined by an ordinary differential equation. Certainly, the radial inhomogeneity and the electric field are included implicitly in averaged values of the coefficients in equation (29). However, evaluation of multiple integrals is incomparably simpler than solving a partial differential equation.

Figure 4 convincingly illustrates the influence of EDF nonlocality on the PC. Here, the dependence (measured in Ref. [94]) of a longitudinal electric field in the PC on the intensity of a longitudinal magnetic field B_z is plotted. Since the field E_z is determined by condition (9) of maintaining a stationarity of PC, it should weaken with an increase in the average lifetime of charged particles. Therefore, with an increase in the strength of a magnetic field which suppresses the radial particle transport, the fraction of electrons in the EDF tail, as well as the field E_z, should decrease. From this point of view, the decline of dependences $E_z(B_z)$, caused by an increase in the ambipolar lifetime (10) with B_z, is absolutely clear. It is observed for such B_z at which the electron transport

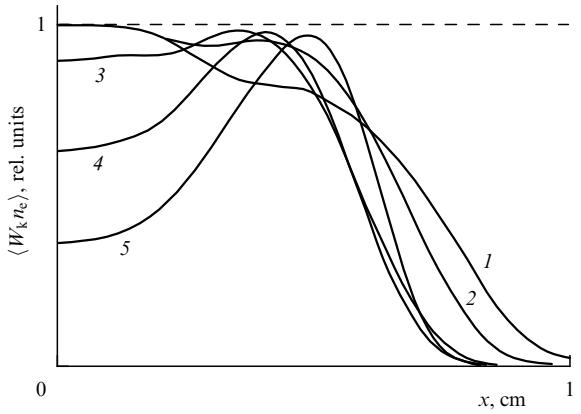

Figure 5. Radial profiles of the total excitation rate of argon atoms in the positive column of a discharge [96, 97] at $E_z = 5$ V cm^{-1}, $p = 3$ Torr, and $-e\varphi(x) = a\varepsilon_1 (x/R)^3$ for various values of a: 0 (dashed line); 0.25 (*1*); 1 (*2*), and 1.5 (*5*).

across the magnetic field becomes much smaller than the ion transport. However, this mechanism that is activated in a relatively strong magnetic field cannot explain the initial portions of the dependences $E_z(B_z)$, where the electric field gets stronger with an increase in the magnetic field strength. These portions are observed for relatively small B_z when the ambipolar diffusion is determined by ions and does not depend on B_z. Estimates show that maximums of the dependences $E_z(B_z)$ correspond to the passage from the nonlocal EDF to a local one; the drop of a completely nonlocal EDF because of inelastic collisions takes place for $\varepsilon > \varepsilon_1$. On the plasma periphery, this corresponds to the kinetic energy $w > \varepsilon_1 + e\varphi(r)$, which is significantly less than ε_1. This means that the peripheral excitation and ionization processes in a nonlocal PC are much more suppressed than in a local PC. In other words, the maximum of the ionization rate in the center for a nonlocal EDF is much sharper than the concentration maximum. Hence, the distance which an ion travels on average between the birthplace and the place of its loss (the wall) and consequently the corresponding times are larger in the nonlocal case than in the local one. Therefore, a somewhat weaker field E_z (increasing with an increase in B_z) is necessary to maintain a stationary nonlocal PC. This view is confirmed by the results of self-consistent calculations [95].

Since the energy relaxation time $(\nu^*)^{-1}$ for the EDF tail is much less than the corresponding time τ_ε for its body, the nonlocality condition with increasing pressure is first violated at large energies, so that the EDF f_0 starts to depend here on ε as well as on the coordinates. Then, an intermediate nonlocality takes place in a sufficiently wide interval of pressures, when only the EDF body depends on the total energy, while its tail is local. In this case, the profiles of excitation rates of atomic levels and consequently the profiles of radiation line intensities, as well as the profiles of excited and metastable particle concentrations, can be nonmonotonic together with other characteristics [96, 97] (Fig. 5).

The physical mechanism underlying this phenomenon can be understood from Fig. 3. The arrival of electrons in the excitation region $\varepsilon > e\varphi + \varepsilon_1$ on the PC axis is caused only by the energy flux Γ_ε, i.e., by Joule heating in a longitudinal field, whereas an additional mechanism is included on the periphery of the PC: an electron can gain energy $\varepsilon > \varepsilon_1$ for $w < \varepsilon_1$ where inelastic impacts are absent, and after that it can move closer to the axis because of spatial diffusion, acquiring the kinetic energy in the radial electric field until it exceeds ε_1, so this electron can proceed to perform an excitation. In other words, such an electron is initially heated by the longitudinal field on the periphery, while its further heating up to $w > \varepsilon_1$ is done by the radial field in its diffusive motion toward the axis. This is a kind of 'diffusion heating' process for such electrons because their differential flux Φ is directed to the axis and the ambipolar field delivers work on them. It is obvious that this phenomenon cannot be reflected in any way within the framework of the traditional hydrodynamic description in which *all* electrons are heated or cooled by the field, whereas in this case the EDF body (for $\varepsilon < \varepsilon_1$) *is cooled* by the ambipolar field, and the tail (for $\varepsilon > \varepsilon_1$) *is heated* by it.

To date, there still exists the problem of the so-called Langmuir paradox, i.e., the reason why in low-pressure PCs,

$$R < \lambda\,, \tag{34}$$

EDFs close to Maxwellian ones are observed. In 1925, Langmuir wrote, "From the complete absence of a kink in the semilogarithmic plot at the wall potential we must conclude that the time of relaxation corresponding to the mechanism by which the electrons acquire their Maxwellian distribution is small compared to the time taken for the electrons to traverse the tube..." [98]. In the concluding 1930 review [99], he repeated, "The mechanism by which these Maxwellian distributions are so quickly established in an ionized gas is not understood... in an ionized gas some additional and more effective agents must be chiefly responsible for the scattering of velocities."

Gabor et al. [62] observed some oscillations in the near-wall region and suggested that these oscillations are responsible for Maxwellization of the EDF. However, up to this day the presence of such oscillations (or at least their universal presence in low-pressure discharges) remains doubtful. In addition, the influence of the oscillations on the EDF is caused by sufficiently complex processes (see, for example, Ref. [77]), so it is absolutely not obvious that precisely they lead to the formation of the Maxwellian EDF.

For example, electrons trapped in the ambipolar potential well cannot reach the plasma periphery and interact with oscillations if the latter are present there. On the other hand, Langmuir's assumption that fast electrons moving away to the wall should lead to a kink in the EDF at $\varepsilon = |e\varphi_{\rm fl}|$ looks too rough in today's context. The point is that the characteristic time of their loss on the wall under condition (34) is not the transit time $\tau_{\rm f} = (R\sqrt{m/e\varphi_{\rm fl}})$ but a much longer time in which the fast electron in elastic scattering gets to the small exit cone. This time, which exceeds even the time ν^{-1} between collisions, tends to infinity at $\varepsilon = |e\varphi_{\rm fl}|$, smoothly decreasing with ε. Thus, the kink in the EDF at $|e\varphi_{\rm fl}|$, corresponding to the boundary between the trapped and transit electrons, is smeared out under condition (34) and its experimental examination presents a difficult problem. It seems plausible that for the complete solution to the problem of the EDF 'Maxwellization' mechanism at low pressures it is necessary first of all [63] to conduct careful experiments in combination with accurate (desirably self-consistent) numerical simulations.

The question of the influence of fast electron loss on the wall and an EDF anisotropy (caused by it) is closely related to the general problem of measuring EDF anisotropy. The applicability of two-term approximation (6) means that the anisotropy caused by the electric field or plasma inhomo-

geneity is small and a power series in spherical harmonics for the EDF converges rapidly.

An important exception is the EDF in the exit cone arising because of fast electron loss on the wall [100, 101]. Electrons with velocities ranging in the exit cone freely leave to the wall from a distance of the order of λ. The symmetrical anticone of the wall losses is empty. It is filled due to elastic collisions. Since the EDF exponentially decreases with an energy increase (in particular, because of electron losses on the wall), most interest is in the electrons with energies not much exceeding $e\varphi_{\rm fl}$:

$$\varepsilon - e\varphi_{\rm fl} \ll \varepsilon\,,\ e\varphi_{\rm fl}\,. \tag{35}$$

Therefore, both the exit cone and the anticone are small. Taking into account this circumstance, it is possible to neglect the scattering of electrons back from these cones into a solid angle corresponding to trapped electrons. Then, the electron kinetic equation also takes the same form (29) as for $\varepsilon < e\varphi$; the only difference is in appearing the additional term $f_0(\varepsilon)\nu_{\rm esc}(\varepsilon)$ on the right-hand side of the equation which takes into account electrons leaving to the exit cone.

The equation describing electrons in the exit anticone for $R \gg \lambda$ is given by

$$\frac{{\rm d}F}{{\rm d}x} = \frac{F - f_0}{\lambda}\,, \tag{36}$$

where F is the EDF in the exit anticone, f_0 is the (almost) isotropic EDF of trapped electrons, and the x-axis coincides with the wall normal. Taking into account that EDF f_0 depends on the coordinate with a large spatial scale, we obtain the solution in the form

$$F(\varepsilon, x) = f_0(\varepsilon)\left(1 - \exp\frac{x}{\lambda}\right). \tag{37}$$

This EDF has a sharp jump at the angle θ_0 corresponding to the boundary of the exit anticone, and the height of the latter exponentially decreases with increasing distance from the wall. The poor convergence of power series in spherical harmonics for EDFs is a consequence of this jump. In the case of a bounded low-pressure plasma, the exit cone corresponding to the right wall overlaps with the anticone to the left one, and vice versa. The EDF anisotropy relating to the exit anticone was observed, for example, in Refs [101–103].

6. Radio-frequency discharges

In radio-frequency (RF) discharges, the electric field usually consists of two components. The RF field heats electrons and forms EDFs. The ion displacement over the RF field period is usually small, so that ion motion is controlled by a stationary (or quasistationary) potential ambipolar field similar to that shown in Fig. 3.

The convincing proof of an EDF nonlocality for capacitive-coupled (CC) RF discharge was obtained in Ref. [104], for surface wave discharge in Ref. [105], and for inductively coupled (IC) discharge in Ref. [106] (Fig. 6).

It should be noted that in the nonlocal case only the coefficient averaged over accessible volume, $\overline{w^{1/2}D_\varepsilon}$, enters Eqn (29) for $f_0(\varepsilon)$. Therefore, even if the energy diffusion coefficient D_ε characterizing the energy deposition is strongly asymmetric, the distributions of the ambipolar potential and the plasma density are symmetric with respect to the discharge center. The small remaining asymmetry is related to the broken nonlocality (see Fig. 2).

The RF field determining $\overline{w^{1/2}D_\varepsilon}(\varepsilon)$ and heating electrons is maximal on the periphery of RF discharges. In IC RF discharges, this is caused by the skin effect. In CC discharges, since the plasma concentration is small on the periphery and the radio-frequency current is conserved, the radio-frequency field heating electrons is the largest here, too. The ambipolar field traps electrons with small energy at the discharge center, so they cannot reach its periphery where the RF field is maximal and the main energy deposition is focused. Therefore, electrons with small ε slowly gain energy in the nonlocal regime from the weak RF field at the center. Since the value of the coefficient $\overline{w^{1/2}D_\varepsilon}(\varepsilon)$ averaged over the accessible cross section, which determines the slope of the EDF $f_0(\varepsilon)$, is small for them, the EDF measured in the discharge center consists of two very different portions. The portion corresponding to small ε describes electrons which cannot reach the region of maximum energy deposition. Therefore, the EDF slope is large for them, and the 'temperature' is small. Electrons with high energy are heated by a strong RF field on the periphery; the EDF slope is much smaller for them. This scenario of the formation of the 'two-temperature' EDFs containing many cold electrons in the central region is illustrated in Fig. 7. The increase in the slope of the EDF tail ($\varepsilon > \varepsilon_1$) caused by the influence of inelastic collisions leads to the formation of the 'three-temperature' EDF.

The electric field in CC RF discharges is potential. It consists of radio-frequency and quasistationary components. In the central region occupied by a quasineutral plasma, both the radio-frequency component $\tilde{E}(r, t)$ heating electrons and the quasistationary ambipolar field are small. A similar situation takes place in the sheath during the plasma phase, when it is 'filled up' by electrons [108]. Since the charged particle concentration decreases from center to periphery, the radio-frequency as well as quasistationary field components in the plasma and in the sheath plasma phase increase toward the periphery. During the volume charge phase, plasma electrons are absent in the sheath. The thickness of the boundary between the plasma and the volume charge, oscillating with the frequency of applied voltage, is on the order of the Debye screening length, and it is small in comparison with the plasma sheath thickness $L_{\rm sh}$ (Fig. 7a). Therefore, electron interactions with this boundary are equivalent to collisions with an oscillating wall [64, 65]. Since the step of random energy walks caused by an electron collision with this moving wall is determined by the velocity of the latter, which is equal to the electron drift velocity at the plasma boundary, the influence of this electron heating mechanism (called stochastic) on the nonlocal EDF can also be described, in principle, by introducing an additional mechanism of diffusion along energy. For this purpose, it is necessary to introduce in kinetic equation (29) an additional term in $\overline{w^{1/2}D_\varepsilon}(\varepsilon)$. The detailed analysis of electron stochastic heating, which is the main mechanism of energy deposition at low pressures and substitutes in this case the Joule heating, can be found in Refs [66, 68, 109, 110]. The stochastic heating in IC discharges is discussed in Refs [66, 109].

The maximum energy deposition on the periphery is characteristic for many discharges. In the case of CC RF discharge, it is caused by the ohmic as well as the stochastic heating of electrons. In the first case, the reason is that, due to the current continuity, the oscillating electric field is maximal

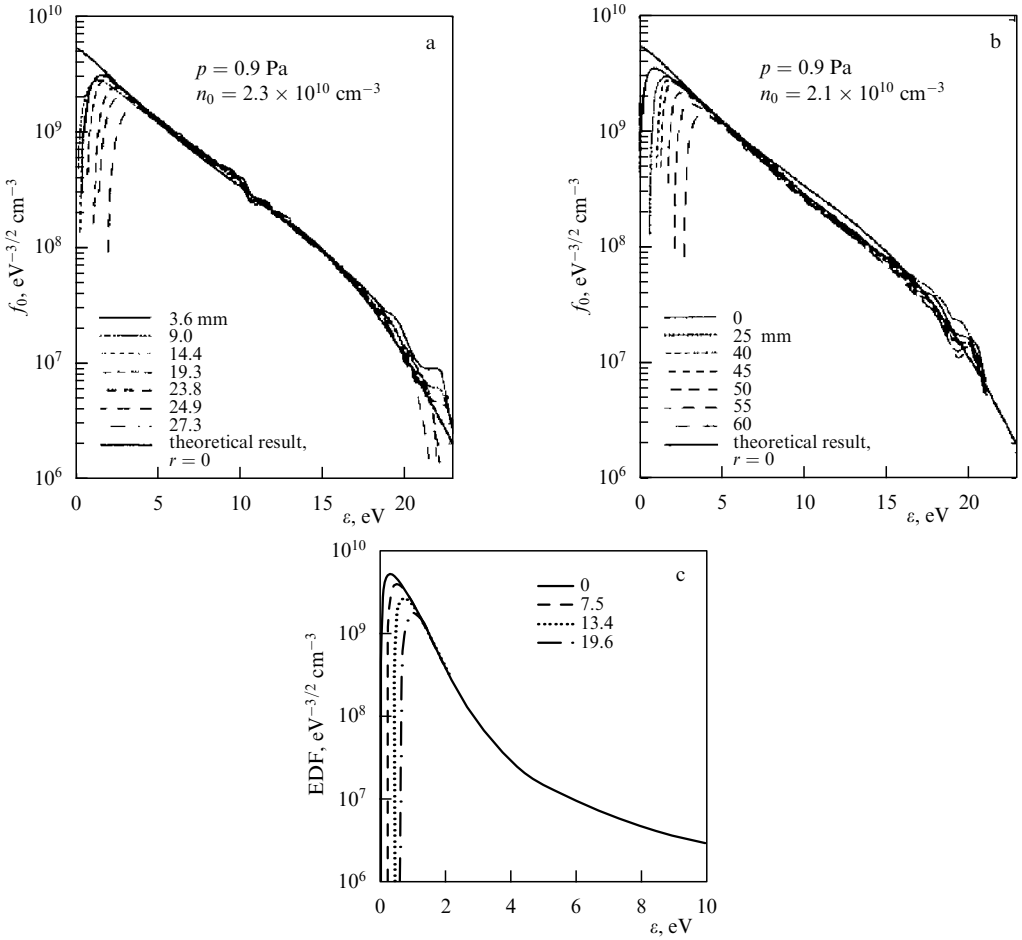

Figure 6. Nonlocal EDFs $f_0(\varepsilon)$ in RF discharges in cylindrical vessels in Ag at 13.56 MHz. (a) CC RF discharge [104]; the distance r [mm] from the middle plane is given for each curve; (b, c) IC RF discharge; EDF along the cylinder axis (b) and in the middle plane for various distances from the axis (c); $L = 6$ cm, and $R = 7.5$ cm [106].

on the periphery where the plasma concentration is small. Therefore, the step of random energy walks (22) is large here, as is the value of D_ε. The stochastic heating [74] also consists in additional random energy walks taking place on the periphery. Consequently, the average of the coefficient $\overline{w^{1/2} D_\varepsilon(\varepsilon)}$ taken over the accessible region rapidly increases with increasing ε (Fig. 7c). In IC RF discharges, the energy deposition is maximum on the periphery because of the skin effect [92, 93, 106].

Similar situations take place in electron-cyclotron resonance (ECR) discharges [111], in surface wave discharges [92, 93], and in discharges near the plasma resonance [109, 112]. For all these cases, formation of a 'two-temperature' EDF with the peak of cold electrons in the discharge center is possible in the nonlocal regime. An example of a CC RF discharge is given in Fig. 8. Similar 'two-temperature' EDFs caused by the skin effect were also observed in an IC RF discharge [107, 113–116].

Self-consistent modeling of a nonlocal IC RF discharge in Ar, combined with its comprehensive experimental investigation, was done in Ref. [105] (see also Refs [107, 113–116]). Here, the 'two-temperature' EDFs containing many slow electrons in the discharge central region were also observed. Agreement between the calculated results and experiment was satisfactory.

If the RF field, which heats electrons, has a sharp maximum with a size less than the mean free path, then the electron energy change in their passage through the field is characterized by weak random pushes. Such a picture takes place in the stochastic heating of electrons in CC or IC RF discharges [64, 65, 74].

In Ref. [107], a simple expression for the energy diffusion coefficient averaged over the accessible volume in the nonlocal case was obtained. Passing through the microwave resonance region, an electron also experiences a push whose strength and sign depend on its phase when entering the resonance region.

Then, the following questions arise: How to express $\Delta\varepsilon$ and v in equation (22) through the field characteristics? How to take an average over the accessible region? What are the conditions for statistically independent consecutive pushes?

The easiest is the collisional case, $L > \lambda$, when an electron collides between two consecutive pushes. Then, correlation disappears between two consecutive pushes experienced by an electron when passing through the resonance region or interacting with a strong field in the volume charge sheath or in the skin layer; the energy acquired by an electron in its push obviously turns into chaotic energy in subsequent collisions with molecules, and in the expression for $w^{1/2} D_\varepsilon$ averaged over the accessible region, the squares of all energies acquired in pushes should be summarized.

For example, if $L \ll \lambda$, then in a CC RF discharge consecutive pushes are statistically independent if the

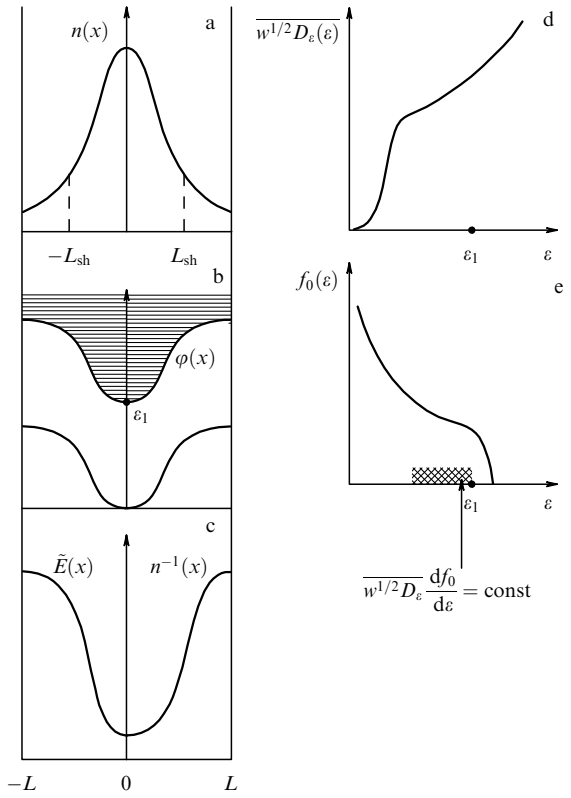

Figure 7. Sketch of dependences in a CC RF discharge [107]. The bell-shaped profiles of plasma concentration (a) lead to the bell-shaped ambipolar potential $\varphi(x)$ (b) and to the bell-shaped profile of the oscillating field strength (c). Since the coefficient $\overline{w^{1/2}D_\varepsilon}(\varepsilon)$ rapidly increases with increasing ε (d), 'two-temperature' or even 'three-temperature' EDFs appear (e).

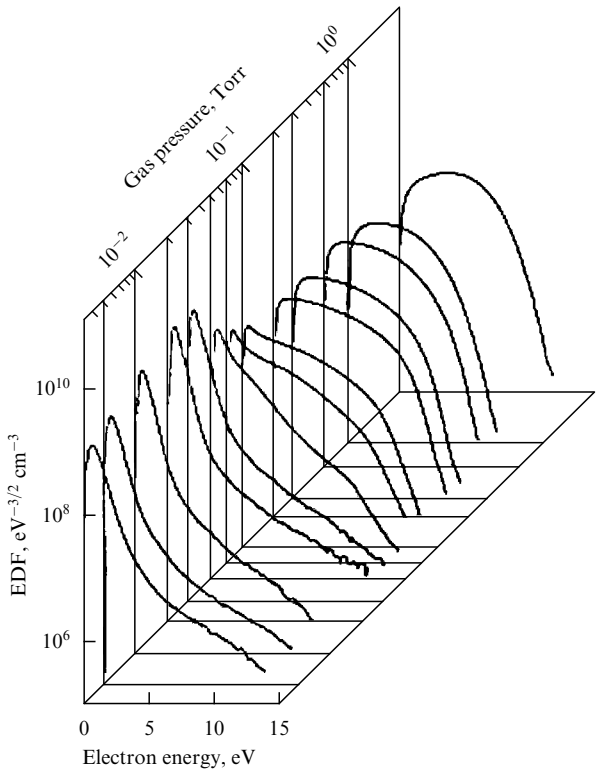

Figure 8. EDFs at various pressures in a CC RF discharge in Ag for $L = 6.7$ cm and $j = 1$ mA cm^{-2} [104].

Chirikov criterion [12] is fulfilled:

$$\frac{\omega L \Delta v}{v^2} > \pi\,, \tag{38}$$

where Δv is the velocity change in a push or in sufficiently frequent collisions, $v > v(\Delta v/\omega L)^{1/2}/L$ (see Ref. [66]). The push-driven Δv is equal to the doubled electron directed velocity at the boundary of the volume charge region, which is much less than the random velocity. Hence, the electron stochastic heating in a CC RF discharge under condition (38) also corresponds to the diffusion along energy. The expression for the energy diffusion coefficient, similar to formulas (18) and (22), can be written as

$$D_\varepsilon^{\text{stoch}}(\varepsilon) = \left\langle (\Delta\varepsilon)^2 \Omega \right\rangle,$$

where $\Omega(\varepsilon, \theta)$ is the bounce frequency of an electron with a total energy ε, and the averaging should be taken over the RF field period and the electron velocity angles. If the size L is small in comparison with the energy relaxation length $\lambda_\varepsilon, \lambda^*$ (26), and the RF field frequency exceeds the corresponding frequency, then the EDF according to equation (29) is determined only by the function of the total energy, $\langle \overline{w^{1/2}D_\varepsilon} \rangle(\varepsilon)$, averaged over the volume and the field period. This function is the sum of the squares of the energy steps which are taken by electrons with the energy ε in all the volume accessible to them in a unit time. Thus, the EDF satisfies the averaged kinetic equation (29) with the replacement of the coefficient $\overline{w^{1/2}D_\varepsilon}(\varepsilon)$ (22) by the sum of two coefficients, namely, the collisional

$$\left\langle \overline{w^{1/2}D_\varepsilon^{\text{coll}}} \right\rangle(\varepsilon) = \frac{\sqrt{m/2}}{6L} \left\langle \int_0^{L(\varepsilon,t)} \frac{e^2 E_{0\omega}^2(x) v^3 \nu(v)}{\omega^2 + \nu^2(v)}\, \mathrm{d}x \right\rangle,$$

and the stochastic

$$\left\langle \overline{w^{1/2}D_\varepsilon^{\text{stoch}}} \right\rangle(\varepsilon) = \int_0^{\theta(\varepsilon)} \left[mv\, V(t) \right]^2 \frac{v^2\sqrt{m/2}}{4\pi L}\, \mathrm{d}(\omega t)\,. \tag{39}$$

Here, $V(t)$ is the velocity of the boundary between the plasma and the volume charge [68], $L(\varepsilon, t)$ is the boundary of the accessible region, $\theta(\varepsilon)$ is the phase during which an electron with energy ε can reach this boundary, and $v(\varepsilon, x) = \sqrt{2(\varepsilon - e\phi(x))/m}$.

Since in both low-pressure CC RF and IC RF discharges the plasma density profiles are bell-shaped and electron heating (collisional as well as stochastic) is concentrated at the periphery, it is a difficult problem to distinguish these mechanisms experimentally. It seems likely that an unambiguous answer to this question requires a detailed quantitative comparison of observed and measured EDFs. For a CC RF discharge, such an attempt was made in Ref. [118] using the model of a step plasma density profile [117]. In this study, rapid EDF leveling-out was observed for high energies, which the authors related to the effect of the electron stochastic heating mechanism. The energy corresponding to the leveling-out origin can be identified with the total energy whose exceeding results in the appearance of electrons which can reach the sheath boundaries and be reflected from the plasma–volume charge boundary.

Convincing evidence of EDF nonlocality is provided by phenomena related to the spatial distribution of discharge

radiation. Thus, the passage from a local to nonlocal EDF with decreasing pressure is accompanied by displacement of the emission maximum from the region of the peak energy deposition to the discharge center, which is shown in Fig. 2. The maximum of the plasma density also moves to the center, and the maxima of the excitation rate and the emission intensity should be sharper than the maximum of the plasma density.

An interesting exception to this rule (that the EDF nonlocality is accompanied by displacements of the excitation rate, emission intensity, and plasma density maxima to the center) is radiation emission from a spherical vessel containing plasma in the transit mode, $R > \lambda$ [107, 119]. In this case, the EDF depends on two variables: the total energy ε and the angular momentum μ, and there are only electrons with small μ in the discharge center. On the other hand, electrons with small momenta μ fall on the wall almost normally, so that if $\varepsilon > e\varphi_{\rm fl}$, where $\varphi_{\rm fl}$ is the wall floating potential, the electrons reside in the 'exit cone' and freely depart towards the wall. The corresponding trajectories are almost empty. Thus, spatial distribution of the emission intensity depends on whether the upper operating level is above or below $e\varphi_{\rm fl}$. Since the EDF for $\varepsilon < e\varphi_{\rm fl}$ depends only on ε, the intensity of lines emitted from a low operating level should be maximal in the center, whereas the line intensities for the upper operating level above $e\varphi_{\rm fl}$ should have a maximum on the periphery and a minimum in the center, especially strongly pronounced for the peripheral mechanism of the energy deposition. These phenomena, as far as we know, have not been observed yet.

7. Cathode region of a direct current discharge

Recently it has become clear that it is impossible to construct a noncontradictory scenario of complex self-consistent nonlocal processes in the near-cathode region of a direct current glow discharge without involving kinetic concepts. Due to historical reasons, this field was traditionally subdivided mainly on the basis of visual features. It was divided into a cathode dark space, negative glow (NG) region, and Faraday dark space (FDS), the latter giving way to a homogeneous or stratified positive column (PC). However, optical characteristics appear as a result of self-consistent interactions of a number of sufficiently complex kinetic and electrodynamic processes; it is therefore more appropriate to base them upon more fundamental kinetic and electric properties and not the radiation characteristics.

First of all, the near-cathode region consists of a quasineutral plasma and positive volume-charge sheaths with a dominant role being played by the cathode sheath. The main portion of the discharge voltage is usually applied to it and electrons are almost absent there. The thickness of the boundary between the cathode sheath and the plasma is of the order of the Debye screening radius — much less than the sheath thickness. Therefore, it is possible to consider it sharp. We restrict ourselves here to the elementary one-dimensional model of an abnormal glow discharge [120]. In this case, two-dimensional phenomena apparently do not play a principal role.

At the cathode surface, $x = 0$, the current is mostly carried by ions, and the densities of electron ($j_{\rm e}$) and ion ($j_{\rm i}$) currents satisfy the equality

$$j_{\rm e}(0) = \gamma j_{\rm i}(0)\,, \qquad (40)$$

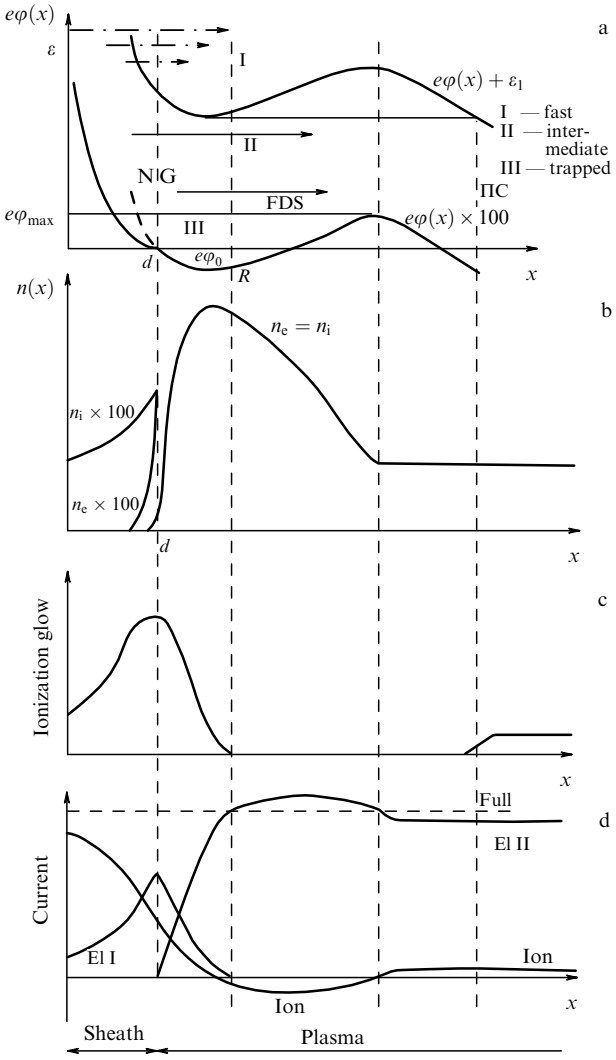

Figure 9. Schematic dependences of plasma parameter profiles in the near-cathode region of a direct current discharge according to Refs [120, 121]. The lower curve in Fig. 9a is the potential profile (the scale of the plasma potential was extended); the upper curve satisfies the relation $\varepsilon = -e\varphi(z_2(\varepsilon)) + \varepsilon_1$. The continuous arrows correspond to intermediate-velocity electrons, and the dash-and-dot arrows to fast electrons.

where $\gamma \ll 1$ is the ion–electron emission coefficient. The electric field in the sheath is strong (Fig. 9a) and the potential drop significantly exceeds ε_1, $\varepsilon_{\rm i}$, so that electrons emitted by the cathode or produced in the sheath are rapidly accelerated and become capable of the ionization and the excitation of molecules. Their number density is small, so that for small x this part of the sheath corresponds to the cathode dark space. Finer radiation details in this region are caused by the behavior of the excitation cross sections. The distribution function of fast electrons with energies much exceeding the excitation and ionization energies is nonlocal, i.e., it is determined not by a local value of E/p but by the whole potential profile of the upstream electron flux. The dash-and-dot arrows in Fig. 9a and the curve El I in Fig. 9d correspond to fast electrons. Their flux exponentially increases in the sheath and reaches its maximum at the plasma boundary. Therefore, an intensive glow already begins within the cathode sheath. Fast electrons penetrate into the plasma, where the field is 2–3 orders of magnitude less than that in the sheath, and cause nonlocal ionization and glow there. The

electrons born near this boundary have a low energy and a small range, so they stop, i.e., they slow down and become incapable of producing ionization and causing glow in the plasma close to its boundary with the cathode sheath.

The fastest electrons emitted directly by the cathode penetrate most deep into the plasma. Thus, the end of their range, $x = R$, is also that point where the negative glow terminates and the FDS originates. Since the fast electron flux is maximal at the plasma boundary, $x = d$, here there are also the maxima of the radiation intensity (Fig. 9c) and ionization rate. Therefore, roughly speaking, half of ionization in the near-cathode region, which transforms the current from ion current (taking place mainly at the cathode) to electron current (dominating in the PC), occurs in the plasma part of the NG.

Thus, NG consists of two parts, where the physical processes are absolutely different. The fast electron flux increases exponentially in the sheath, so that the part of the NG belonging to the sheath occupies only a small region adjacent to the plasma boundary. The length of this region is of the order of the length where the fast electron flux increases essentially. Ionization in the plasma part of NG, where the field is weak or even reversed, is also quite considerable. The length of the plasma part is determined by the range of fastest electrons emitted by the cathode. This simple model developed in Refs [120, 121] contradicts the traditional paradigm according to which the ionization is determined by a local field, and it is therefore possible only in the sheath where the electric field is strong.

According to the Townsend condition of maintaining a stationary discharge, the number of ions created by an electron emitted from a cathode should be equal to γ^{-1}. In other words, ions born in the sheath as well as in the plasma part of the NG should return to the cathode. The ions produced in the sheath are easily taken out to the cathode by the strong volume-charge field. However, the ion current from the plasma part of the NG region, which makes a significant portion of the total current, can be transported only due to the weak ambipolar diffusion mechanism. This is possible only if there is a very large concentration gradient in a plasma. Since the NG length is fixed, the plasma concentration in it should be very high. Then, near the NG end there is a peak of plasma concentration, exceeding its PC value by more than an order of magnitude (Fig. 9b). For $x > R$, the FDS originates. The electron diffusion current from the region of a peak plasma concentration, directed towards the anode, significantly exceeds the total current, so that the ambipolar field near the concentration maximum should form a potential well for electrons. Therefore, the reverse field region is located in the direction from the concentration maximum to the anode. In a sufficiently long discharge tube, plasma concentration in this region decreases to a value corresponding to that in the PC, and at the FDS end there is a maximum of the potential $e\varphi_{\max}$ and the second field reverse point (Fig. 9a) corresponding to the passage to the PC.

For such a potential profile, the EDF naturally breaks up into three groups separated by sharp boundaries. The first one (I) is represented by fast electrons with energies significantly exceeding the excitation energy ε_1 and the ionization energy ε_i. These electrons are responsible for ionization and emission in the near-cathode region. In an NG plasma, fast electrons are only an insignificant fraction of the full electron concentration, and in the FDS they are not present at all; therefore, probe measurements in the sheath are difficult and their probe diagnostics are less promising. Radiation intensity profiles can give abundant information on fast electrons.

The third group (III) consists of trapped electrons with energies below the potential $e\varphi_{\max}$ of the second field reverse point (or the anode potential in a short discharge). These electrons do not participate in the current flow, so their only energy sources are collisions with neutral particles and extremely rare collisions of the second kind with excited particles and a few electrons of two other groups. Since trapped electrons are the main fraction of the electron population in NG plasma, their EDF is Maxwellian with a temperature slightly exceeding room temperature, and consequently the potential and their concentration are linked by the Boltzmann relation. Therefore, the characteristic scale of the FDS potential is room temperature, and the potential difference $\varphi_{\max} - \varphi_0$ in this region is insignificant in comparison with ε_1 and ε_i, whereas the plasma density change can be rather significant.

It is for the same reason that the question of the reverse field in NG and FDS remained debatable for a long time. The point is that the achievement of an accuracy exceeding 1 eV in probe discharge measurements remains to be difficult. Therefore, some authors (beginning with J J Thomson [122]) reported the presence of a reverse field, while others (see, for example, Ref. [123]) did not observe it. Currently, reasons similar to the above were confirmed by field measurements of the Stark effect in highly excited states [124] as well as by numerous numerical simulations, so that the presence of the reverse field in the FDS is no longer questioned.

The second group (II) is represented by intermediate electrons with energies

$$e\varphi_{\max} < \varepsilon < e\varphi_0 + \varepsilon_1 .$$

Until the intermediate electrons reach the PC, their kinetic energy is insignificant, so their energy relaxation is only caused by very small energy losses in elastic collisions with atoms. Neglecting such processes, the EDF of these electrons is given by a simple expression similar to formula (32):

$$f_0^{\text{int}}(\varepsilon) = \Phi(\varepsilon) \int_z^{z_2(\varepsilon)} \frac{\mathrm{d}x'}{w^{1/2} D(\varepsilon, x')} , \qquad (41)$$

where $\Phi(\varepsilon)$ is the differential flux. The reason for the FDS formation is clearly seen from Fig. 9: there are just no electrons with $w > \varepsilon_1$, since the fast ones have already slowed down, and the intermediate electrons have not accelerated yet.

The presence of three groups of electrons near the cathode was already reported by Langmuir [61]. Detailed investigation of the EDF in the near-cathode region using Langmuir's procedure was done by Emeléus and coworkers [125–128]. These groups were initially classified as primary, secondary, and ultimate groups. However, a viewpoint closer to the current one was expressed in Ref. [127], according to which the fast group corresponds to electrons accelerated in the cathode drop, "...We have concluded that fast electrons, which will be referred to without implication as to their origin as primary electrons, are really present." Interpretation of two groups of slower electrons by the authors of Ref. [127] and their definition of the boundary between them were more vague. It is also necessary to note that EDFs for all three groups were *ad hoc* assumed by them to be Maxwellian.

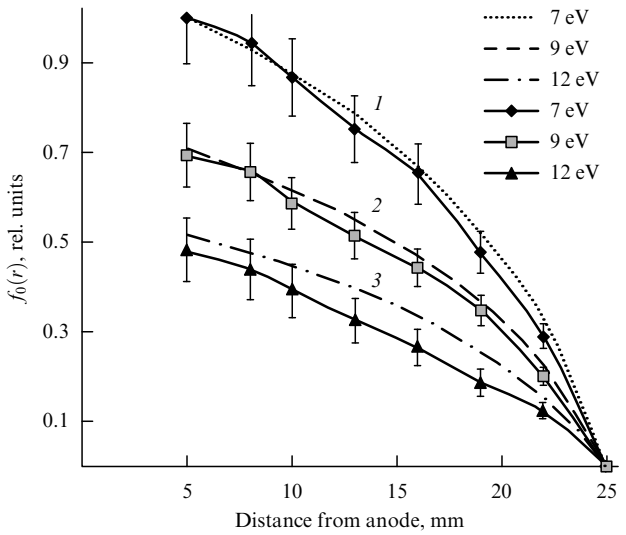

Figure 10. EDF of intermediate electrons (II) in He for different values of the total energy [129].

As far as we know, the only convincing illustration of an EDF in the FDS looking like expression (41) was obtained in Ref. [129] for a magnetized plasma discharge in crossed fields with a confined Hall drift. A distinction between trapped electrons with Maxwell–Boltzmann distribution and intermediate ones was also observed there. Figure 10 gives a comparison of the measured EDF of intermediate electrons with that calculated according to expression (41).

8. Anode region of a direct current discharge

A closed self-consistent theory of the anode region of a direct current discharge is lacking. However, it is obvious that its construction is also impossible without an adequate account of electron kinetics.

The main subject of Langmuir's interest was relatively high-current arcs in which the EDF is close to a Maxwellian one. Therefore, Langmuir used the expression

$$j = en_0 \sqrt{\frac{8T_e}{\pi m}} \exp \frac{e\varphi}{T_e} \tag{42}$$

for the electron current density at an electrode being at the potential φ, placed in the plasma, which corresponds to the Maxwell–Boltzmann EDF. Since the total current is small in comparison with the chaotic electron current $en_0\sqrt{8T_e/(\pi m)}$, the electrode potential $e\varphi$ with respect to the plasma should be negative and significantly exceed T_e. Therefore, the anode potential should exceed by a few T_e/e the floating potential at which the ion and electron currents are equal:

$$\varphi_{fl} = -\frac{T_e}{e} \ln \sqrt{\frac{M}{m}}. \tag{43}$$

However, depletion of the EDF tail responsible for the anode current is considerable enough, even for the current values used by Langmuir. Therefore, values of φ, φ_{fl} should actually be essentially smaller than those given by expressions (42), (43). For example, the values of φ_{fl} observed and obtained from self-consistent kinetic calculations are given in Fig. 11. From this figure we notice that the discrepancy is rather significant.

Since the number of fast electron losses on the wall in a stationary discharge should be equal to the number of ionizations, with both inelastic collisions and wall losses leading to an exponential decrease in the EDF with increasing energy, the effective ionization potential ε_i should be close to φ_{fl}. Otherwise, it would be impossible to equilibrate these loss rates of fast electrons. If, for example, the value of $e\varphi_{fl}$ were much less than ε_i, the EDF-tail electron loss on the wall would lead to an exponentially small ionization rate insufficient to maintain the discharge, and vice versa [130].

This scenario corresponds to a negative voltage drop in the anode sheath, though a significantly smaller one than that given by expression (5). In this case, the ionization and excitation in the cathode sheath should be strongly suppressed, so that the anode region should be dark. Meanwhile, a positive anode voltage drop and a bright thin film adjacent to the anode surface are also often observed [125, 126, 131, 132]. Roughly speaking, the anode potential with respect to the plasma is negative for large currents, and for small currents it is positive.

A model of the anode positive drop was formulated by von Engel [133], and the kinetic approach was developed in Ref. [134]. In this case, the EDF looks like expressions (32), (41), and $\Phi(\varepsilon) = \text{const}$. Such EDFs depleted with slow

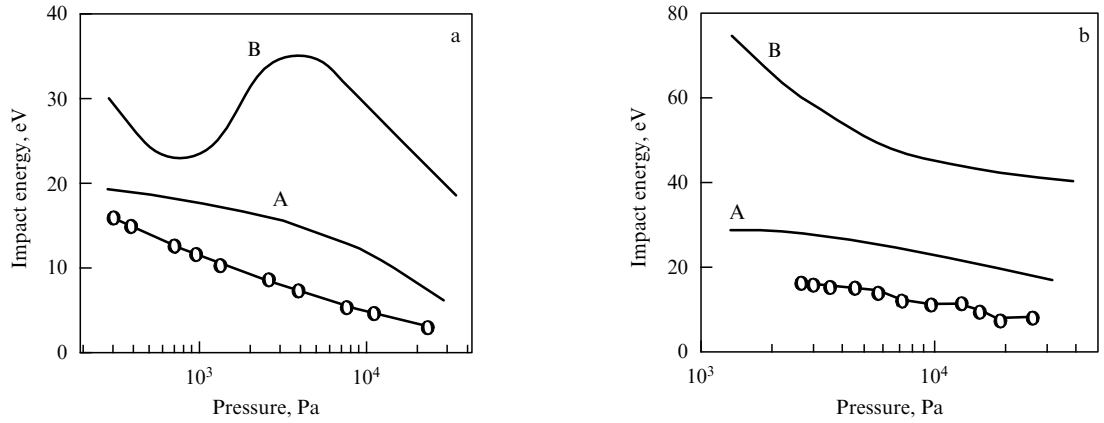

Figure 11. Energy of Ag (a) and He (b) ions falling on an isolated wall in an IC RF discharge [92, 93]. This energy is close to the floating potential $e\varphi_{fl}$. The curves A were calculated by using a nonlocal EDF; the curves B correspond to the floating potential (43) for the values of T_e equal to 2/3 of the average electron energy.

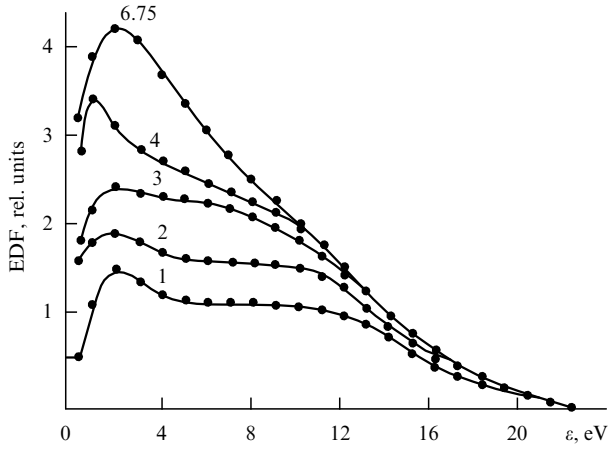

Figure 12. EDFs at different distances from the anode (quoted alongside the curves in cm) in Ne, measured at a pressure of 1 Torr, current 19 mA, and tube radius 1.4 cm. The length of the region where the EDF portion is depleted with slow electrons equals $\varepsilon_1/(eE_z) = 6.75$ cm.

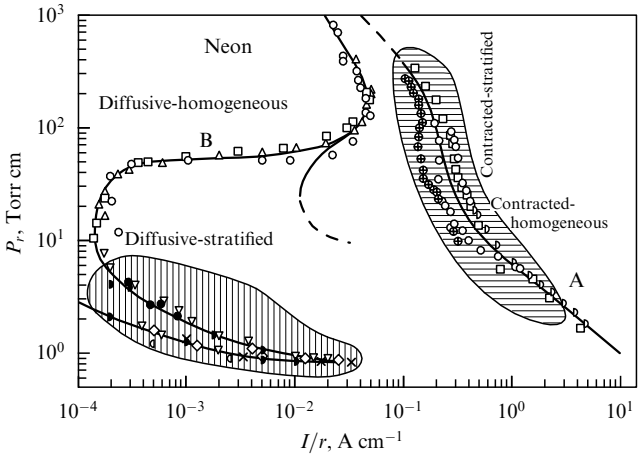

Figure 13. Domains of existence for traveling striations of various types in Ne according to Ref. [138].

electrons were observed in Ref. [135]. The length of the plasma region perturbed by the anode presence appears to be rather large. It is equal to $\varepsilon_1/(eE_z)$. The electron distribution functions here, shown in Fig. 12, satisfactorily agree with those calculated according to formula (41). The reason why this perturbed region was ignored for such a long time lies, apparently, in the fact that the EDF tail responsible for ionization and radiation emission appears almost unperturbed here, and therefore this region cannot be visually separated from the positive column.

9. Striations

Since a glow-discharge plasma is far away from thermodynamic equilibrium, numerous instabilities show their worth in it. At the nonlinear stage, the instabilities can develop to spatially nonuniform and/or nonstationary ordered structures, i.e., can lead to various forms of discharge self-organization. Various types of instabilities were considered, for example, in Refs [136, 137]. The most well-known instabilities among those caused by kinetic ionization phenomena are striations and discharge constriction. Here, we consider striations whose relation (for their elementary types) to electron kinetics has already been reliably established.

Because standing striations (longitudinal periodic stationary glowing sheaths in a direct current discharge) are easily visible to the naked eye, the history of their investigation, in essence, coincides with the history of studying the glow discharge itself. Observation of a visually homogeneous PC with the help of a rotating mirror revealed long ago that running striations appeared there very often. Therefore, an opinion was expressed that this stratified form, instead of a homogeneous form, is typical for PCs (Fig. 13). As a result of persistent work over almost two centuries, huge experimental material on the striation properties has been accumulated, as presented, in particular, in Refs [139–144].

The level of understanding of this interesting phenomenon is still quite far from perfect. A huge variety of striation types, complex dependences of their characteristics on discharge conditions, as well as a deficiency of data on the ionization kinetics, make the search for explanation of striations a sufficiently difficult problem. An additional obstacle was that researchers, naturally, searched for a uniform mechanism of striation occurrence for a long time. Therefore, almost all types of plasma waves were considered as possible candidates for this mechanism. Only by the 1960s it became clear that striations represent a phenomenon inherent in nonequilibrium gas-discharge plasma where the dominant role is played by processes of generation and transport of charged particles. Therefore, striations, and especially traveling striations, are often called ionization waves as well. We shall confine ourselves to considering below the ionization waves in noble gases which were studied experimentally in most detail; the first steps in theoretical understanding of this phenomenon were taken also in this direction.

Existence domains of traveling striations are displayed in Fig. 13. The upper current boundary A was found by Pupp [145]. Properties of ionization waves in Ag for parameters close to this boundary were carefully investigated by Wojaczek [146–149]. In the whole region between boundary A and lower boundary B, the positive column is stratified. Outside the existence domain of spontaneous striations, near its boundary, weakly damped ionization waves can be excited by an external action on PC.

It is seen from Figs 13 and 14 that for a large current (horizontally shaded area in Fig. 13) the striations of one type only are found in PC, with parameters smoothly depending on discharge conditions.

For a small current, the situation is significantly more difficult in the neighborhood of boundary B. Waves of three various types are observed: S-, P-, and R-striations. Their main feature is that for striations of one type the potential drop across the striation is approximately constant (see Table 1). This relation is called Novak's rule [150]. For S-striations, this potential drop is close to the ionization potential ε_i (for noble gases ε_i is close to the excitation energy ε_1 of the first atomic level), and for P-striations it is close to its half. The voltage across an R-striation lies between these values. These facts combined with a complex EDF behavior in striations [72] explicitly testify that kinetic phenomena play an important role here.

First attempts to analyze the PC ionization instability, whose nonlinear stage appears as observable striations, were made within the framework of the hydrodynamic approach.

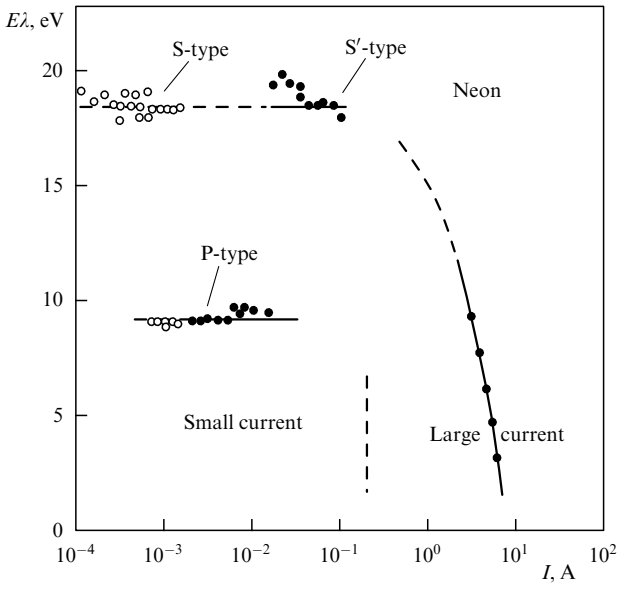

Figure 14. Parameters of spontaneous striations in Ne [138]. It is seen that Novak's rule is well satisfied for small current [150].

Let us consider a field perturbation in an inhomogeneous current-carrying plasma. The longitudinal current, more than 99% of which is transferred by electrons, can be expressed as

$$j_z = e\left(-n_e\,\mu_e E_z + D_e\,\frac{dn_e}{dz}\right). \tag{44}$$

From the current conservation in a plasma whose homogeneous concentration $n_e^{(0)}$ has a small addition $\tilde{n}_e(z,t)$, it follows that the inhomogeneous addition $\tilde{E}_z(z,t)$ to the field, $E_z = E_z^{(0)} + \tilde{E}_z(z,t)$, contains two components:

$$\tilde{E}_z = \tilde{E}_z^{(c)} + \tilde{E}_z^{(d)}(z,t) = -E_z^{(0)}\,\frac{\tilde{n}_e}{n_e^{(0)}} - \frac{T_e}{en_e^{(0)}}\,\frac{d\tilde{n}_e}{dz}\,. \tag{45}$$

For large-scale perturbations with the wave number k satisfying the inequality $k < eE_z/T_e$, the first, current, component dominates in expression (45). This means that the longitudinal field E_z in plasma constrictions, which heats up electrons and forms EDF, is less than the equilibrium value $E_z^{(0)}$ corresponding to the balance between ionization processes and loss of charged particles. Since in the hydrodynamic approximation the field weakening in the constrictions leads to reduction of the electron temperature T_e and the ionization rate depends on T_e exponentially, in the long-wave plasma constrictions the ionization rate drops rapidly. Therefore, such perturbations can be unstable only under rather exotic conditions, so they hardly correspond to such a common phenomenon as the formation of striations.

On the other hand, the properties of short-wave perturbations with $K = kT_e/(eE_z) \gg 1$ are determined not by local balances of particles and energies but, first and foremost, by electron transport processes. The main part of the perturbation $\tilde{E}_z$ is the ambipolar field $\tilde{E}_z^{(d)}$ which compensates for the electron diffusion. For sinusoidal perturbation of the density, $\tilde{n}_e$, the field perturbation $\tilde{E}_z^{(d)}$ is shifted by $\pi/2$ to the cathode with respect to $\tilde{n}_e$ and its relative value is $\sim K$ times more than $\tilde{n}_e$.

The perturbation $\tilde{T}_e$ is mainly determined by the balance between the electron Joule heating due to the diffusion field $\tilde{E}_z^{(d)}$ proportional to $\tilde{n}_e$ ($\sim K\tilde{n}_e$) and the electron thermal conductivity proportional to $\tilde{T}_e$ ($\sim K^2\tilde{T}_e$), as a result of which the relative value of the perturbation $\tilde{T}_e$ is $\sim K$ times *less* than $\tilde{n}_e$. Values of perturbed plasma parameters (reduced to their equilibrium values) and phase shifts between them are depicted in Fig. 15.

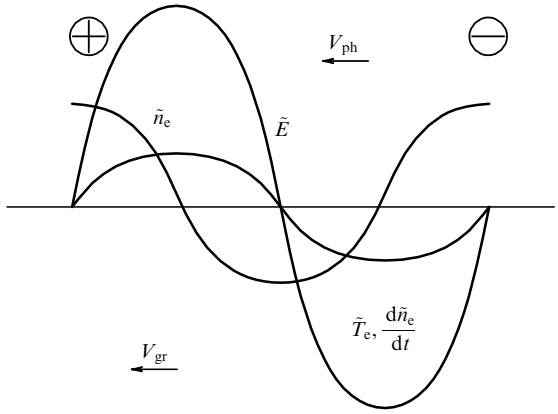

Figure 15. Values of relative perturbations in an ionization wave for large currents and phase shifts between them.

Sinusoidal perturbation of the ionization frequency Z, caused by the dependence of Z on T_e, is also shifted to the cathode by $\pi/2$ with respect to $\tilde{n}_e$, thus corresponding to the wave propagating to the cathode. Its dispersion law takes the form [151–153]

$$\omega = Z\,\frac{d\ln Z/d\ln T_e - 1}{aK}\,, \tag{46}$$

where a is the dimensionless coefficient of the electron thermal conductivity. The same expression (without derivation) was given by Wojaczek [149] as an approximation of experimental data.

Since perturbation $\tilde{T}_e$ decreases with K, the phase velocity $V_{ph} = \omega/k$ also decreases with K. At the same time, the group velocity $V_{gr} = d\omega/dk$ is directed to the anode and is equal to the phase velocity in this approximation. The rate of the wave growth or decay and, consequently, the instability mechanism are related to the imaginary part of the wave frequency, which is a small correction to dispersion law (46). In conditions of Ref. [149], the instability is caused by the dependence $Z(n_e)$ related to the influence of interelectron collisions on the EDF tail. If the plasma density is so high that even the EDF tail is Maxwellian, the dependence $Z(n_e)$ disappears and the ionization waves become damped. Hence, the EDF body (which corresponds to a much longer relaxation time than that of the EDF tail) is Maxwellian near the upper current boundary A (see Fig. 13) and the hydrodynamic description of electrons is applicable. Then, kinetic phenomena can be taken into account in this case by the dependence $Z(n_e, T_e)$. In other words, dispersion law (46) and the ionization wave damping are determined here by hydrodynamics, whereas to evaluate their increments and thus determine the possibility of their instability it is merely sufficient to take advantage of the local electron kinetics.

Agreement between the simple one-dimensional model [151, 152] and experiment [146–149] reflected in the horizontally shaded area A in Fig. 13 has turned out to be unexpectedly good, as can be seen from Figs 16 and 17.

However, attempts to apply this approach even to the PC in the same gas and tube but at different values of the current (and from Fig. 13 it can be seen that striations are observed at

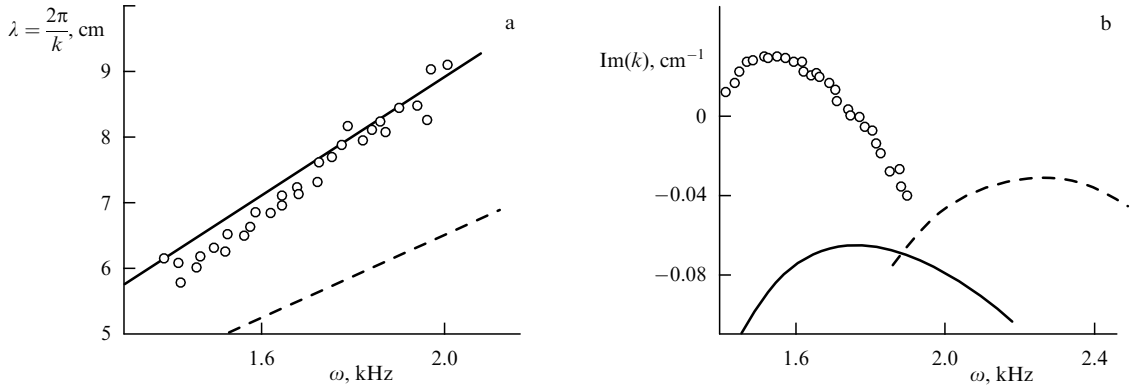

Figure 16. The dispersion law (a) and the spatial increment (b) for traveling striations in Ag near the Pupp upper boundary. Dashed lines correspond to formula (46), and solid lines take account of PC's two-dimensional character [151, 152]. Conditions correspond to a PC at $Rp = 0.8$ Torr cm, $I/R = 2.2$ A cm^{-1}, and $R = 1.65$ cm. In calculations, the approximation $\nu(w) \sim w^{3/2}$ for the transport collisional frequency was accepted.

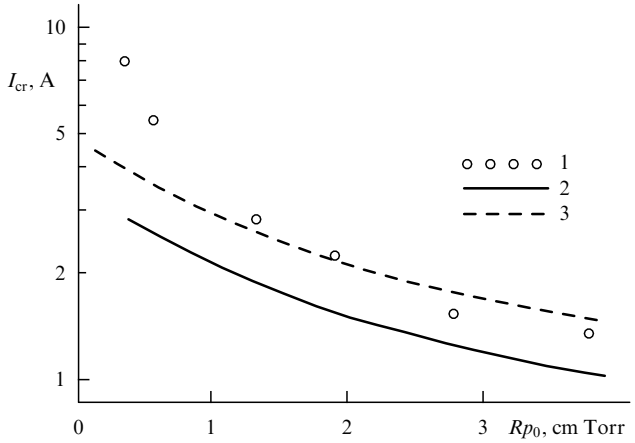

Figure 17. The upper current boundary for the existence domain of spontaneous traveling striations [145] in Ar. Notations and experimental conditions are the same as in Fig. 16. Curves correspond to vanishing the imaginary part of the frequency.

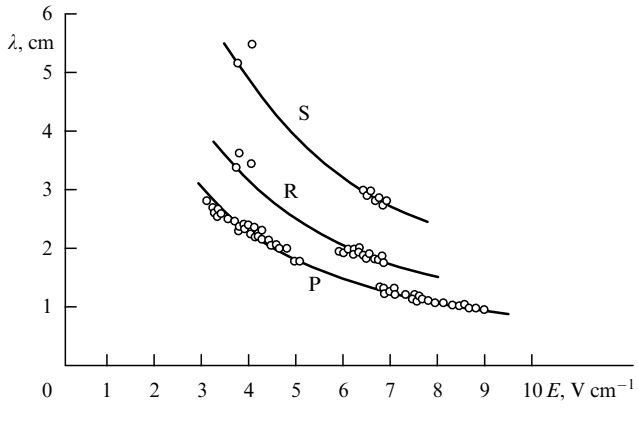

Figure 18. The wavelengths of traveling striations in Ne according to Ref. [143].

Table 1. Values of the product $E_z\lambda$ for type P-, R-, and S-striations at small currents [143].

	P	R	S	ε_1	ε_i
He	14.2	—	30.05	19.8	24.6
Ne	9.2	12.67	19.48	16.62	21.5
Ar	6.7	9.5	12.0	11.55	15.76

currents three orders of magnitude smaller than currents in the area A) came across serious difficulties.

First, the above scenario does not contain even a hint of the presence of resonant wavelengths or Novak's rule (Figs 14 and 18).

Values of product $E_z\lambda$ for striations of various types at small currents [143] are given in Table 1. The electric field induced in S- and P-striations is presented in Fig. 19.

The second problem concerns the instability mechanism. Clearly, for current values orders of magnitude lower than those corresponding to the Pupp upper boundary no influence of interelectron collisions on the EDF can be discussed, and therefore the instability mechanism should be totally different.

The third difficulty appears because of the condition $K \gg 1$, which means that the wavelength should be less than the electron energy relaxation length. However, the latter length is on the order of or less than the relaxation length for the EDF body. Therefore, the hydrodynamic description of short-wave inhomogeneities is possible *only* for large currents when interelectron collisions are frequent enough to at least make the EDF body Maxwellian at energies below ε_1. Therefore, deeper analysis of electron kinetics is necessary to describe striations at small currents.

It was noted in Ref. [154] that in the single-level approximation the response of 'pipeline' EDF (32) to a small spatially periodic field perturbation feature resonant properties: it is maximal if the potential drop across the spatial field period is equal to ε_1/p, where $p = 1, 2, \ldots$.

This fact immediately brings to mind S- and P-striations; the physical mechanism of these resonances as a manifestation of EDF bunching effect in the (ε, x) plane is discussed in Refs [155, 156]. For the elementary case of S-striations, this effect is illustrated in Fig. 20.

In the single-level approximation, EDF (32) corresponds to the stairs with the step height equaling ε_1. Ignoring the contribution from elastic collisions to the electron energy balance, the distance between different stairs does not depend on z and is equal to the distance between them at the point of creation or injection of electrons. An account of the small (on the order of $\kappa = m/M(l/\lambda)^2 \ll 1$, where l is the step length) contribution of elastic collisions and the energy which an electron loses when coming down one step of the stairs leads to two effects. First, the steps of a stair EDF (see Fig. 20)

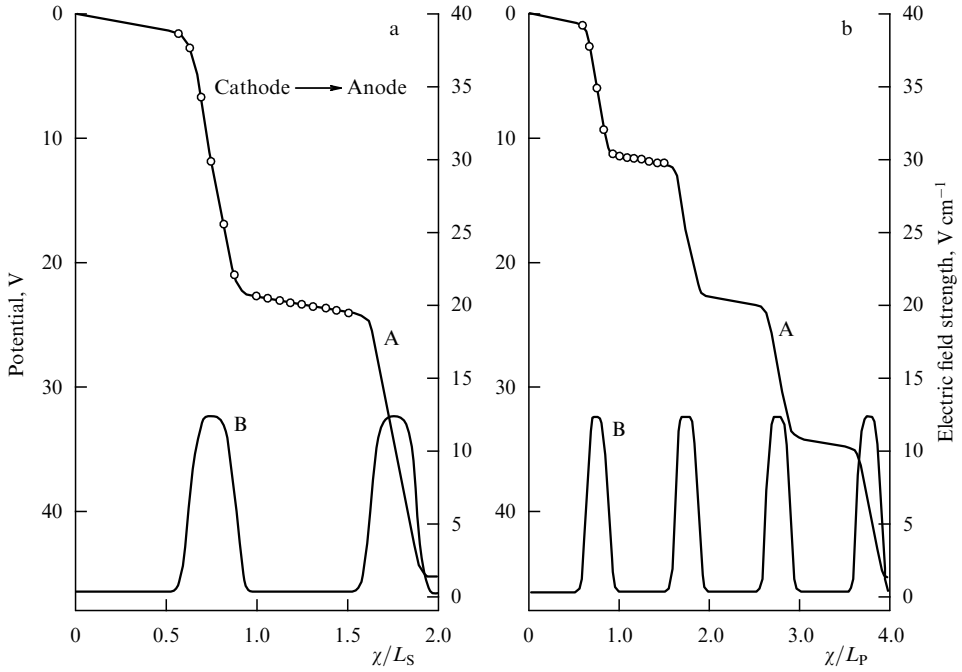

Figure 19. The potential (A) and longitudinal field E_z (B) profiles in S-striations (a) and P-striations (b) [157]; the coordinate is quoted in units of the striation length.

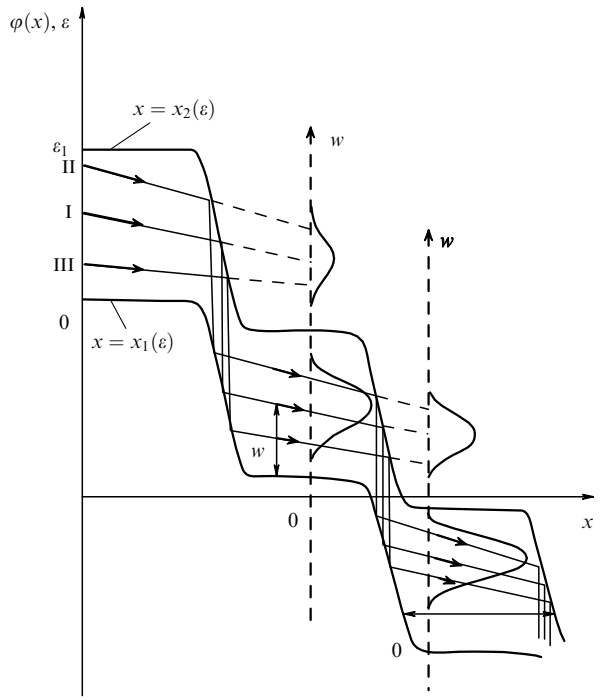

Figure 20. EDF bunching in a spatially periodic electric field. 'Stairs' I corresponds to the resonant electron trajectory. An electron proceeding along it, having experienced an inelastic collision and having lost energy ε_1, appears at the symmetrical point in the (ε, x) plane and remains on the same trajectory. The curve $x = x_1(\varepsilon)$ represents the potential profile; the curve $x = x_2(\varepsilon)$ is the boundary of an area where inelastic impacts take place, $w(\varepsilon, x_2(\varepsilon)) = \varepsilon_1$. Since a small energy loss usually increases with a kinetic energy increase in elastic collisions, trajectories II and III approach trajectory I. EDFs of the kinetic energy at various points are shown separately.

become slightly sloping. Therefore, the kinetic energy of electrons proceeding along the stair trajectory II decreases faster than that for trajectory III. Hence, trajectories I and II come closer to resonant trajectory I. For electrons came down $N \gg 1$ steps, this convergence of trajectories is proportional to κN.

The second effect is that since energy loss in collisions (including elastic ones) is a stochastic process, the steps of a stair EDF gradually spread out. This spreading is on the order of $\kappa\sqrt{N}$. For $N \gg 1$, such a spreading is negligibly small in comparison with the first effect (with the difference of energy losses on different steps). Calculations show [158] that the EDF bunching effect takes place beyond the single-level model as well as when accounting for interelectron collisions that are not so frequent.

Thus, this effect brings to mind electron bunching in a klystron. A spatially periodic electric field with a potential difference in its period, slightly exceeding ε_1 (by a fraction of $\sim \kappa$), acts on the EDF as a klystron with respect to energy, spanning differential fluxes to resonant trajectory I. Any EDF injected into such a field contracts near trajectory I into a delta-shaped distribution.

An equation for differential flux $\Phi(\varepsilon)$ (21) was derived in Refs [155, 156]:

$$\Phi(\varepsilon) = \Phi\big[\varepsilon - \varepsilon_1(1 + \kappa A)\big] + \kappa\Phi(\varepsilon)\,\frac{\mathrm{d}\Psi(\varepsilon)}{\varepsilon_1\,\mathrm{d}\varepsilon} + \kappa^2 B\,\frac{\mathrm{d}^2\Phi}{\varepsilon_1^2\,\mathrm{d}\varepsilon^2}\,, \tag{47}$$

where the constants A and B as well as function $\Psi(\varepsilon)$ are on the order of unity. Function $\Psi(\varepsilon)$ describes the dependence of the average energy loss rate in elastic collisions on ε. By dividing the ε-axis into segments of length $\varepsilon_1(1 + \kappa A)$ and considering the segment number N and energy ε within the section as two independent variables, equation (47) describes mapping [77] in the (ε, N) plane. In Refs [155, 156], it was also shown that a spatially periodic field with a potential drop (in the period) which slightly (by $\sim \kappa/p$) differs from ε_1/p also leads to EDF bunching at integer values of p. This

corresponds to S-striations ($p = 1$) and P-striations ($p = 2$). For $p = 1$, there is only one resonant value on the unit interval ε, so that the steady EDF is periodic in ε with a period close to ε_1. For P-striations ($p = 2$), two resonant trajectories, Φ_1 and Φ_2, are found, and in the black wall approximation (for large cross sections of inelastic collisions) these values do not equal each other and are determined by the EDF shape as $z \to -\infty$. The period of P-striations in this case is also close to $\varepsilon_1(1 + \kappa A)$. It decreases twofold only when $\Phi_1 = \Phi_2$.

The nature of R-striations remained mysterious until it was shown [157] that any rational values of $p = q/r$ can also lead to EDF bunching. It appeared that observed R-striations correspond to $p = 3/2$. In a series of studies by Winkler and coworkers [159–161] and Golubovskii and coworkers [157, 162, 163], the one-dimensional kinetic equation was numerically solved in a given periodic spatially modulated field without the black wall approximation. In calculations as well as in experiments [157, 162, 163], it was specifically revealed that the period of R-striations in this case is close to $\varepsilon_1(1 + \kappa A)2$, whereas $\Phi_1 = \Phi_2$.

EDFs observed in S-, P-, and R-striations also agree well with this pattern. However, unlike S-striations ($p = 1$) and P-striations, steady R-striations have two resonant trajectories corresponding to various values Φ_1, Φ_2 of the differential flux. It should be noted, however, that a self-consistent theory of S-, P-, and R-striations is still lacking. It is also not clear whether striations corresponding to other values of p are actually possible.

Thus, striations represent a new type of synergetic objects in which self-organization appears not on the hydrodynamic [164] but on the kinetic level.

10. Conclusion

Sometimes there are statements that all basic physical phenomena and mechanisms of gas discharges can be understood, at least qualitatively, on the basis of the plasma hydrodynamic description, while a kinetic analysis is extremely time-consuming and is necessary only at the quantitative level for an exact evaluation of discharge parameters, determining breakdown voltages and exact values of kinetic coefficients, etc. It follows from the above examples that electron kinetics, which appeared on the basis of Langmuir probe diagnostics, constitutes today one of the main components in the modern physics of gas discharges [15, 153, 165]. Without adequately taking it into account, even a qualitative understanding of a variety of basic discharge phenomena, such as spatial profiles of ionization and radiation intensity, and striations, is impossible.

The author is deeply grateful to R Franklin for the encouraging advice. This work was supported by RFBR (project 09-02-01194a).

References

1. Maxwell J C *Philos. Trans. R. Soc. Lond.* **170** 231 (1879)
2. Maxwell J C *Cambr. Philos. Soc. Trans.* **12** 547 (1879)
3. Maxwell J C *The Scientific Papers* Vol. 2 (Cambridge: Univ. Press, 1890) pp. 713–741
4. Boltzmann L *Wien. Ber.* **66** 275 (1872)
5. Boltzmann L *Vorlesungen über Gastheorie* (Leipzig: J.A. Barth, 1910–1912) [Translated into English: *Lectures on Gas Theory* (Berkeley, Calif.: Univ. of California Press, 1964); translated into Russian (Moscow: GITTL, 1953)]
6. Lifshitz E M, Pitaevskii L P *Fizicheskaya Kinetika* (Physical Kinetics) (Moscow: Nauka, 1979) [Translated into English (Oxford: Pergamon Press, 1981)]
7. Gurevich L E *Osnovy Fizicheskoi Kinetiki* (The Foundations of Physical Kinetics) (Leningrad–Moscow: Gostekhteoretizdat, 1940)
8. Lorentz H A *The Theory of Electrons and Its Applications to the Phenomena of Light and Radiant Heat* (Leipzig: B.G. Teubner, 1909) [Translated into Russian (Moscow: GITTL, 1953)]
9. Chapman S, Cowling T G *The Mathematical Theory of Non-Uniform Gases* 2nd ed. (Cambridge: Univ. Press, 1952) [Translated into Russian (Moscow: IL, 1960)]
10. Enskog D *Svensk. Vet. Akad. Arkiv. Math. Ast. Fys.* **16** 1 (1921)
11. Landau L D *Zh. Eksp. Teor. Fiz.* **16** 574 (1946); *J. Phys. USSR* **10** 25 (1946)
12. Sagdeev R Z, Usikov D A, Zaslavsky G M *Nonlinear Physics: from the Pendulum to Turbulence and Chaos* (New York: Harwood Acad. Publ., 1988)
13. Alexandrov A F, Bogdankevich L S, Rukhadze A A *Osnovy Elektrodinamiki Plazmy* (Principles of Plasma Electrodynamics) (Moscow: Vysshaya Shkola, 1988) [Translated into English (Berlin: Springer-Verlag, 1984)]
14. Biberman L M, Vorob'ev V S, Yakubov I T *Kinetika Neravnovesnoi Nizkotemperaturnoi Plazmy* (Kinetics of Nonequilibrium Low Temperature Plasmas) (Moscow: Nauka, 1982) [Translated into English (New York: Consultants Bureau, 1987)]
15. Smirnov B M *Fizika Slaboionizovannogo Gaza v Zadachakh s Resheniyami* 2nd revised ed. (Physics of Weakly Ionized Gases (Problems and Solutions)) (Moscow: Nauka, 1988) [Translated into English (Moscow: Mir Publ., 1981)]
16. Mitchner M, Kruger Ch H (Jr.) *Partially Ionized Gases* (New York: Wiley, 1973) [Translated into Russian (Moscow: Mir, 1976)]
17. Langmuir I, Mott-Smith H *General Electric Review* **27** (1924); in *The Collected Works of Irving Langmuir* Vol. 4 (Ed. Ch G Suits) (Oxford: Pergamon Press, 1960)
18. Jeans J H *Dynamical Theory of Gases* 2nd ed. (Cambridge: Univ. Press, 1916)
19. Loeb L B *Kinetic Theory of Gases* 2nd ed. (New York: McGraw-Hill, 1934)
20. Loeb L B *Basic Processes in Gaseous Electronics* (Berkeley, Calif.: Univ. of Calif. Press, 1955)
21. Townsend J (Sir) *Electrons in Gases* (London: Hutchinson's Sci. and Tech. Publ., 1948)
22. Engel A, Steenbeck M *Electrische Gasenladungen, ihre Physik und Thechnick* (Berlin: J. Springer, 1932–1934) [Translated into Russian (Moscow–Leningrad: ONTI, 1935)]
23. Druyvesteyn M J *Physica* **10** 61 (1930)
24. Druyvesteyn M J *Physica* **1** 1003 (1934)
25. Druyvesteyn M J *Physica* **3** 65 (1936)
26. Druyvesteyn M J, Penning F M *Rev. Mod. Phys.* **12** 87 (1940)
27. Cravath A M *Phys. Rev.* **36** 248 (1930)
28. Cravath A M *Phys. Rev.* **46** 332 (1934)
29. Davydov B *Phys. Z. Sowjetunion* **8** 59 (1935)
30. Davydov B *Phys. Z. Sowjetunion* **9** 433 (1936)
31. Morse P M, Allis W P, Lamar E S *Phys. Rev.* **48** 412 (1935)
32. Healey R H, Reed J W *The Behavior of Slow Electrons in Gases* (Sydney: Amalgamated Wireless, 1941)
33. Loeb L B *Fundamental Processes of Electrical Discharge in Gases* (New York: J. Wiley, 1939)
34. Smit J A *Physica* **3** 543 (1936)
35. Schottky W *Phys. Z.* **25** 342 (1924)
36. Schottky W *Phys. Z.* **25** 635 (1924)
37. Schottky W *Phys. Rev.* **28** 74 (1926)
38. Holstein T *Phys. Rev.* **70** 367 (1946)
39. Margenau H *Phys. Rev.* **69** 508 (1946)
40. Margenau H *Phys. Rev.* **73** 297 (1948)
41. Allis W P, in *Handbuch der Physik* Vol. 21 (Ed. S Flügge) (Berlin: Springer, 1956) p. 383
42. Brown S, in *Handbuch der Physik* Vol. 22 (Ed. S Flügge) (Berlin: Springer, 1956) p. 531
43. MacDonald A D *Microwave Breakdown in Gases* (New York: Wiley, 1966) [Translated into Russian (Moscow: Mir, 1969)]
44. Ginzburg V L, Gurevich A V *Usp. Fiz. Nauk* **70** 201 (1960); **70** 393 (1960) [*Sov. Phys. Usp.* **3** 115 (1960); **3** 175 (1960)]

45. Gurevich A V, Shvartsburg A B *Nelineinaya Teoriya Rasprostraneniya Radiovoln v Ionosfere* (Nonlinear Theory of Radio Wave Propagation in Ionosphere) (Moscow: Nauka, 1973)
46. Shkarofsky J P, Johnston T W, Bachynski M P *The Particle Kinetics of the Plasmas* (Reading, Mass.: Addison-Wesley Publ. Co., 1966) [Translated into Russian (Moscow: Atomizdat, 1969)]
47. Tsendin L D *Zh. Tekh. Fiz.* **47** 1598 (1977) [*Sov. Phys. Tech. Phys.* **22** 925 (1977)]
48. Bernstein I B, Holstein T *Phys. Rev.* **94** 1475 (1954)
49. Tsendin L D *Zh. Eksp. Teor. Fiz.* **66** 1638 (1974) [*Sov. Phys. JETP* **39** 805 (1974)]
50. Tsendin L D, Golubovskii Yu B *Zh. Tekh. Fiz.* **47** 1839 (1977) [*Sov. Phys. Tech. Phys.* **22** 1066 (1977)]
51. Tsendin L D *Zh. Tekh. Fiz.* **48** 1569 (1978) [*Sov. Phys. Tech. Phys.* **23** 890 (1978)]
52. Wiesemann K *Ann. Physik* **478** 275 (1969)
53. Dreicer H *Phys. Rev.* **115** 238 (1959)
54. Dreicer H *Phys. Rev.* **117** 329 (1960)
55. Gurevich A V *Zh. Eksp. Teor. Fiz.* **39** 1296 (1960) [*Sov. Phys. JETP* **12** 904 (1961)]
56. Lebedev A N *Zh. Eksp. Teor. Fiz.* **48** 1393 (1965) [*Sov. Phys. JETP* **21** 931 (1965)]
57. Babich L P *High-Energy Phenomena in Electric Discharges in Dense Gases* (Arlington, Va: Futurepast, 2003)
58. Nikandrov D S *Zh. Tekh. Fiz.* **78** (12) 35 (2008) [*Tech. Phys.* **53** 1565 (2008)]
59. Tsendin L D *Pis'ma Zh. Tekh. Fiz.* **35** (22) 40 (2009) [*Tech. Phys. Lett.* **35** 1044 (2009)]
60. Gurevich A V, Zybin K P *Usp. Fiz. Nauk* **171** 1177 (2001) [*Phys. Usp.* **44** 1119 (2001)]
61. Langmuir I *Phys. Rev.* **26** 585 (1925)
62. Gabor D, Ash E A, Dracott D *Nature* **176** 916 (1955)
63. Kudryavtsev A A, Tsendin L D *Zh. Tekh. Fiz.* **69** (11) 34 (1999) [*Tech. Phys.* **44** 1290 (1999)]
64. Godyak V A *Zh. Tekh. Fiz.* **41** 1364 (1972) [*Sov. Phys. Tech. Phys.* **16** 1073 (1972)]
65. Godyak V A *IEEE Trans. Plasma Sci.* **34** 755 (2006)
66. Kaganovich I D, Polomarov O V, Theodosiou C E *IEEE Trans. Plasma Sci.* **34** 696 (2006)
67. Buddemeier U, Kaganovich I D, in *Electron Kinetics and Applications of Glow Discharges* (NATO ASI Ser., Ser. B, Vol. 367, Eds U Kortshagen, L D Tsendin) (New York: Plenum, 1998) p. 283
68. Lieberman M A, Godjak V A *IEEE Trans. Plasma Sci.* **26** 955 (1998)
69. Boyd R L F, Twiddy N D *Proc. R. Soc. Lond. A* **250** 53 (1959)
70. Boyd R L F, Twiddy N D *Proc. R. Soc. Lond. A* **259** 145 (1960)
71. Rayment S W, Twiddy N D *J. Phys. D* **2** 1747 (1969)
72. Rayment S W *J. Phys. D* **7** 871 (1974)
73. Eidmann K *Beitr. Plasmaphys.* **21** 99 (1971)
74. Godyak V A *Soviet Radio Frequency Discharge Research* (Falls Church, VA: Delphic Associates, 1986)
75. Fedorov V L *Zh. Tekh. Fiz.* **55** 926 (1985) [*Sov. Phys. Tech. Phys.* **30** 554 (1985)]
76. Woods R C, Sudit I D *Phys. Rev. E* **50** 2222 (1994)
77. Golubovskii Yu B, Zakharova V M, Pasunkin V N, Tsendin L D *Fiz. Plazmy* **7** 620 (1981) [*Sov. J. Plasma Phys.* **7** 340 (1981)]
78. Arslanbekov R R, Khromov N A, Kudryavtsev A A *Plasma Sources Sci. Technol.* **3** 528 (1994)
79. Kagan Yu M, in *Spektroskopiya Gazorazryadnoi Plazmy* (Spectroscopy of Gas Discharge Plasma) (Exec. Ed. S E Frish) (Leningrad: Nauka, 1970) p. 201
80. Kagan Yu M, Perel' V I *Usp. Fiz. Nauk* **81** 409 (1963) [*Sov. Phys. Usp.* **6** 767 (1964)]
81. Nighan W L *Phys. Rev. A* **15** 1701 (1977)
82. Nighan W L *Phys. Rev. A* **16** 1209 (1977)
83. Wagner E B, Davis F J, Hurst G S *J. Chem. Phys.* **47** 3138 (1967)
84. Lowke J J, Parker J H (Jr.) *Phys. Rev.* **181** 302 (1969)
85. Aleksandrov N L, Napartovich A P, Starostin A N *Fiz. Plazmy* **6** 1123 (1980) [*Sov. J. Plasma Phys.* **6** 618 (1980)]
86. Aleksandrov N L, Son E E, in *Khimiya Plazmy* (Plasma Chemistry) Vol. 7 (Ed. B M Smirnov) (Moscow: Atomizdat, 1980) p. 35
87. Mahoney L J et al. *J. Appl. Phys.* **76** 2041 (1994)
88. Wendt A E et al., in *Electron Kinetics and Applications of Glow Discharges* (NATO ASI Ser., Ser. B, Vol. 367, Eds U Kortshagen, L D Tsendin) (New York: Plenum Press, 1998) p. 489
89. Allis W P, Haus H A *J. Appl. Phys.* **45** 781 (1974)
90. Mümken G, Schlüter H, Tsendin L D *Phys. Rev. E* **60** 2250 (1999)
91. Tsendin L D *IEEE Trans. Plasma Sci.* **34** 728 (2006)
92. Kortshagen U *Phys. Rev. E* **49** 4369 (1994)
93. Kortshagen U, in *Electron Kinetics and Applications of Glow Discharges* (NATO ASI Ser., Ser. B, Vol. 367, Eds U Kortshagen, L D Tsendin) (New York: Plenum Press, 1998) p. 329
94. Deutsch H, Pfau S *Beitr. Plasmaphys.* **16** 87 (1976)
95. Uhrlandt D, Winkler R *IEEE Trans. Plasma Sci.* **29** 462 (2001)
96. Tsendin L D, Bogdanov E A, Kudryavtsev A A *Phys. Rev. Lett.* **94** 015001 (2005)
97. Bogdanov E A, Kudryavtsev A A, Tsendin L D *IEEE Trans. Plasma Sci.* **34** 834 (2006)
98. Langmuir I *Phys. Rev.* **26** 585 (1925)
99. Compton K T, Langmuir I *Rev. Mod. Phys.* **2** 123 (1930)
100. Yamamoto N et al. *Phys. Rev. A* **13** 1543 (1976)
101. Ishijima T, Uenuma M, Tsendin L D, Sugai H, *XVI ESCAMPIG, Grenoble, 2002* Vol. 1, p. 221, poster 2-7
102. Godyak V, Alexandrovich B, Rahman B, in *2006 59th Annual Gaseous Electronics Conf., GEC-2006, October 10 – 13, 2006, Columbus, Ohio, USA*
103. Godyak V, private communication
104. Godyak V A, Piejak R B *Phys. Rev. Lett.* **65** 996 (1990)
105. Kortshagen U *J. Phys. D* **26** 1691 (1993)
106. Kortshagen U, Pukropski I, Tsendin L D *Phys. Rev. E* **51** 6063 (1995)
107. Tsendin L D *IEEE Trans. Plasma Sci.* **34** 728 (2006)
108. Raizer Yu P, Shneider M N, Yatsenko N A *Vysokochastotnyi Emkostnoi Razryad* (Radio Frequency Capacitive Discharge) (Moscow: Izd. MFTI. Fizmatlit, 1995); *Radio-frequency Capacitive Discharges* (Boca Raton: CRC Press, 1995)
109. Aliev Yu M, Schlüter H, Shivarova A *Guided-Wave-Produced Plasmas* (Berlin: Springer, 2000)
110. Kaganovich I D, Polomarov O V, Theodosiou C E *Phys. Plasmas* **11** 2399 (2004)
111. Greene D G S, Shohet J L *Plasma Phys.* **15** 5 (1973)
112. Vas'kov V V, Gurevich A V, Dimant Ya S *Zh. Eksp. Teor. Fiz.* **84** 536 (1983) [*Sov. Phys. JETP* **57** 310 (1983)]
113. Kortshagen U, Pukropski I, Zethoff M *J. Appl. Phys.* **76** 2048 (1994)
114. Mümken G, Kortshagen U *J. Appl. Phys.* **80** 6639 (1996)
115. Kortshagen U *J. Vac. Sci. Technol. A* **16** 300 (1998)
116. Kortshagen U, Heil B G *IEEE Trans. Plasma Sci.* **27** 1297 (1999)
117. Orlov K E, Smirnov A S *Plasma Sources Sci. Technol.* **8** 37 (1999)
118. Tatanova M et al. *Plasma Sources Sci. Technol.* **18** 025026 (2009)
119. Tsendin L D *Plasma Sources Sci. Technol.* **12** S51 (2003)
120. Kolobov V I, Tsendin L D *Phys. Rev. A* **46** 7837 (1992)
121. Kudryavtsev A A, Morin A V, Tsendin L D *Zh. Tekh. Fiz.* **78** (8) 71 (2008) [*Tech. Phys.* **53** 1029 (2008)]
122. Thomson J J *Philos. Mag. 6* **18** 441 (1909)
123. Pringle D H, Farvis W E J *Proc. Phys. Soc. B* **68** 836 (1955)
124. Gottscho R A et al. *Phys. Rev. A* **40** 6407 (1989)
125. Emeléus K G *Proc. Cambr. Philos. Soc.* **23** 531 (1927)
126. Emeléus K G, Harris N L *Philos. Mag. 7* **4** 49 (1927)
127. Emeléus K G, Brown W L *Philos. Mag. 7* **7** 17 (1929)
128. Emeléus K G, Brown W L, Cowan H McN *Philos. Mag. 7* **17** 146 (1934)
129. Platonov A A, Slyshov A G, Tsendin L D, Wagner S D *Zh. Tekh. Fiz.* **76** (7) 22 (2006) [*Tech. Phys.* **51** 841 (2006)]
130. Kudryavtsev A A, Tsendin L D *Pis'ma Zh. Tekh. Fiz.* **28** (20) 7 (2002) [*Tech. Phys. Lett.* **28** 841 (2002)]
131. Klyarfeld B N, Neretina N A *Zh. Tekh. Fiz.* **28** 296 (1959)
132. Klyarfeld B N, Neretina N A *Zh. Tekh. Fiz.* **29** 15 (1959)
133. von Engel A *Philos. Mag. 7* **32** 417 (1941)
134. Tsendin L D *Zh. Tekh. Fiz.* **56** 279 (1986)
135. Al-Havat Sh, Golubovskii Yu B, Tsendin L D *Zh. Tekh. Fiz.* **57** 1285 (1987) [*Sov. Phys. Tech. Phys.* **32** 760 (1987)]
136. Napartovich A P, Starostin A N, in *Khimiya Plazmy* (Plasma Chemistry) Vol. 6 (Ed. B M Smirnov) (Moscow: Atomizdat, 1979) p. 153

137. Velikhov E P, Kovalev A S, Rakhimov A T *Fizicheskie Yavleniya v Gazorazryadnoi Plazme* (Physical Phenomena in Gas Discharge Plasma) (Moscow: Nauka, 1987)
138. Pfau S, Rutscher A, Wojaczeck K *Beitr. Plasmaphys.* **9** 333 (1969)
139. Garscadden A "Ionization waves in glow discharges", in *Gaseous Electronics* Vol. 1 (Eds M N Hirsh, H J Oskam) (New York: Academic Press, 1978) p. 65
140. Oleson N L, Cooper A W *Adv. Electronics Electron Phys.* **24** 463 (1968)
141. Nedospasov A V *Usp. Fiz. Nauk* **94** 439 (1968) [*Sov. Phys. Usp.* **11** 174 (1968)]
142. Nedospasov A V, Hait V D, *Kolebaniya i Neustoichivosti Nizkotemperaturnoi Plazmy* (Oscillations and Instabilities in Low-Temperature Plasma) (Moscow: Nauka, 1979)
143. Pekarek L *Usp. Fiz. Nauk* **94** 463 (1968) [*Sov. Phys. Usp.* **11** 188 (1968)]
144. Kolobov V I *J. Phys. D* **39** R487 (2006)
145. Pupp W *Phys. Z.* **33** 844 (1932)
146. Wojaczek K *Beitr. Plasmaphys.* **1** 30 (1960)
147. Wojaczek K *Beitr. Plasmaphys.* **2** 15 (1962)
148. Wojaczek K *Beitr. Plasmaphys.* **5** 307 (1965)
149. Wojaczek K *Beitr. Plasmaphys.* **6** 319 (1966)
150. Novak M *Czech. J. Phys.* **10** 954 (1960)
151. Tsendin L D *Zh. Tekh. Fiz.* **39** 1341 (1969) [*Sov. Phys. Tech. Phys.* **14** 1013 (1969)]
152. Tsendin L D *Zh. Tekh. Fiz.* **40** 1600 (1970) [*Sov. Phys. Tech. Phys.* **15** 1245 (1971)]
153. Raizer Yu P *Fizika Gazovogo Razryada* (Gas Discharge Physics) 2nd ed. (Moscow: Nauka, 1992) [Translated into English (Berlin: Springer, 1997)]
154. Rohlena K, Ruzicka T, Pekarek L *Czech. J. Phys. B* **22** 920 (1972)
155. Tsendin L D *Fiz. Plazmy* **8** 169 (1982) [*Sov. J. Plasma Phys.* **8** 96 (1982)]
156. Tsendin L D *Fiz. Plazmy* **8** 400 (1982) [*Sov. J. Plasma Phys.* **8** 228 (1982)]
157. Golubovskii Yu B et al. *Phys. Rev. E* **72** 026414 (2005)
158. Shveigert V A *Fiz. Plazmy* **15** 1230 (1989) [*Sov. J. Plasma Phys.* **15** 714 (1989)]
159. Sigeneger F, Winkler R *Contrib. Plasma Phys.* **36** 551 (1996)
160. Sigeneger F et al. *Plasma Chem. Plasma Process.* **18** 153 (1998)
161. Sigeneger F, Winkler R *Plasma Chem. Plasma Process.* **20** 429 (2000)
162. Golubovskii Yu B et al. *Zh. Tekh. Fiz.* **67** (9) 14 (1997) [*Tech. Phys.* **42** 997 (1997)]
163. Golubovskii Yu B et al. *Phys. Rev. E* **68** 026404 (2003)
164. Haken H *Synergetics* (Berlin: Springer-Verlag, 1978) [Translated into Russian (Moscow: Mir, 1980)]
165. Golubovskii Yu B et al. *Kinetika Elektronov V Neravnovesnoi Gazorazryadnoi Plazme* (Kinetics of Electrons in Nonequilibrium Gas Discharge Plasma) (St. Petersburg: Izd. SPbGU, 2004)